Received February 20, 2021; revised March 16, 2021; accepted April 6, 2021. Date of publication 8 April 2021; date of current version 16 April 2021.

Digital Object Identifier 10.1109/OJCOMS.2021.3071853

Effective Collaboration to Maximize Throughput Based on Multiuser Cooperative Mobility in Social-Physical Ad Hoc Networks

JIQUAN XIE [1] (Graduate Student Member, IEEE), AND TUTOMU MURASE [2] (Member, IEEE)

[1]Graduate School of Informatics, Nagoya University, Nagoya 464-8601, Japan

[2]Information Technology Center, Nagoya University, Nagoya 464-8601, Japan

CORRESPONDING AUTHOR: J. XIE (e-mail: xiejq@net.itc.nagoya-u.ac.jp)

This work was supported in part by ROIS NII Open Collaborative Research under Grant 2020-20S1202 and Grant 2021-21S1203; and in part by the Grants-in-Aid for Scientific Research under Grant 19H04093, Grant 20H00592, and Grant 21H03424.

ABSTRACT Social networks are playing an increasingly important role in information dissemination in wireless ad hoc networks with the wide adoption of the mobile Internet. In particular, in social application scenarios such as Facebook and Twitter, the questions of how to fully consider the social relationships between users to ensure the quality of service (QoS) urgently needs to be explored. This paper investigates an optimal social relay selection scheme with high intimacy requirements to maximize the system throughput for social-physical ad hoc networks with device-to-device (D2D) communication. Different from previous studies, we jointly consider feasible relays and multiuser cooperative mobility with satisfactory link reliability for throughput maximization. On the one hand, we formulate a nonlinear and nonconvex problem, which is typically NP-hard, for throughput optimization. Specifically, this optimization problem is divided into two subproblems: i) selecting the optimal relays and ii) determining the best mobility strategy in terms of throughput. On the other hand, we first convert the relay selection subproblem into an optimal stopping phase problem, and then propose a definition of a graph representing the degrees of interference between physical links, transforming the original optimization problem into a convex problem that is solvable using the Lagrange multiplier method. Based on the above, we propose the Relay selection and Link Interference Degree Graph (RS-LIDG) algorithm to solve the two subproblems. Numerical simulations verify that the proposed RS-LIDG method improves the throughput gain by 26.29%, 123.43%, and 236.47% compared to the intuitive method (IM), the social-trust-based random mobility selection method (STS-RM), and the physical-based random mobility selection method (PHS-RM), respectively.

INDEX TERMS Social network, wireless ad hoc networks, throughput, relay selection, multiuser cooperative mobility.

I. INTRODUCTION

In recent years, users have been able to roam with Internet of Things (IoT) devices anytime and anywhere by virtue of the widespread deployment of 5th-Generation (5G) networks. However, the current 5G technology has many limitations, such as the high power consumption of base stations and terminal devices [1]. Device-to-Device (D2D), with its advantages of noncentralization and light power consumption, is an essential complement to 5G technology. The IEEE 802.11 standard presents ad hoc network as an indispensable class of local area networks [2] that can be widely adopted in small-scale environments and communities, such as meeting rooms, exhibition halls, and hotels.

Due to the intrinsic properties of IoT devices, resource factors such as transmission power, bandwidth, and coverage are often subject to constraints when implementing applications with high quality of service (QoS) and low latency requirements [3]. With the proliferation of smartphones and

social applications, efforts to meet their users' increasing demands in established ad hoc networks are becoming an important focus of research. System throughput is a vital criterion for judging the user experience to ensure that QoS requirements are met. Generally, the system throughput is defined as the amount of data traffic per unit slot received by the access point (AP). In addition, with the widespread popularity of various ubiquitous mobile and wearable devices in the IoT context, choosing such a device as temporary relay may lead to data integrity and privacy concerns. The peer-to-peer relay selection process is crucial for D2D-assisted IoT operations. At present, social attributes have also become a non-negligible factor in IoT design since IoT device users' behavior will significantly affect performance. As the underlying driver of the social attributes among users, intimacy is consequently becoming an essential measure of social networks' stability [4]. Therefore, we seek to construct network architectures that can simultaneously satisfy demands for high QoS, high intimacy, and strong link reliability in existing networks.

Traditional research has focused on increasing bandwidth, enhancing transmission power, or improving the efficiency of medium access control (MAC) layer communication protocols to increase system throughput [5]. Unfortunately, these schemes always require high consumption of infrastructure resources and rarely consider social attributes such as intimacy. To date, researchers have presented several mechanisms of relay selection with comprehensive consideration of both social demands and throughput. Zhang *et al.* [6] proposed a socially aware relay selection mechanism based on optimal stopping theory, which provides a significant throughput gain compared with the direct transmission method. Pan and Wang [7] introduced a distance-based relay selection mechanism that considers only different relay locations within a certain proximity. In regard to social-trust and physical-based integration schemes, Fang and Li [8] demonstrated that a hybrid scheme outperformed the methods of [9] and [10] in most scenarios. Furthermore, Zhang *et al.* [11] proposed a joint social-physical relay reselection mechanism based on [6] and proved that the proposed scheme achieves a trade-off between the selection time and sufficient data traffic. However, for most of the above methods, only time-division multiple access (TDMA) communication systems, with a high selection time and poor throughput performance have been analyzed. Currently, an effective collaboration scheme that can achieve both high throughput and a low relay selection cost in practice has not yet been proposed.

In this paper, a relay selection scheme and a multiuser cooperative mobility strategy are employed to ensure link reliability and stability in terms of physical link (high throughput) and social link (good intimacy). Our previous work [12], [13] has illuminated that collaborative user behavior in cooperative mobility without social impacts can yield significant gains with low resource costs in system throughput compared to traditional approaches. To the best of our knowledge, in the context of social-physical ad hoc networks, we are the first to comprehensively consider an optimal scheme based on both relay selection and a multiuser cooperative mobility strategy to address the above issue. The contributions of this paper are summarized as follows:

- We model a social-physical network based on multiuser cooperative mobility and formulate a throughput maximization problem that specifies the requirements for both the social and physical layers. In detail, we define the concept of link reliability by jointly considering both social intimacy and the probability of successful data transmission. A nonlinear and nonconvex (NCNL) optimization problem is then constructed, which is a classical NP-hard problem.
- We propose the Relay Selection and Link Interference Degree Graph (RS-LIDG) algorithm. The original optimization problem is decomposed into two subproblems: a relay selection scheme and a multiuser cooperative mobility strategy. For the relay selection scheme, it is demonstrated that high intimacy is achieved first while ensuring cooperation, and then optimal stopping theory is used to select the user who maximizes the effective transmission time as the optimal relay.
- We creatively exploit graph theory and prove that the nonconvex problem can be transformed into a convex one by iteratively partitioning the mobility region to find the optimal locations of the mobile relays. In the multiuser cooperative mobility strategy, the relays' different locations and the interference between users are jointly considered. Simulation results show that the proposed RS-LIDG algorithm can achieve a significant throughput gain and a reduction in relay selection time compared to previous methods.

The rest of the paper is organized as follows. Section II discusses related work, and we then present the system model in Section III. In Section IV, the throughput optimization problem is formulated. We propose the RS-LIDG algorithm in Section V, and analytical results are reported in Section VI. Finally, the conclusion and future work are presented in Section VII.

II. RELATED WORK

This section briefly introduces the related work on relay selection schemes and user cooperative mobility to improve throughput.

A. RELAY SELECTION SCHEMES

We highlight the differences between this paper and related works [6]–[11]. The related works on relay selection schemes are summarized in Table 1. The previous schemes can be classified into three categories. Category I corresponds to the intuitive method [9], while category II contains schemes based on only social trust [6] or only physical considerations [7]. Category III comprises a hybrid scheme [8], [10]

TABLE 1. Summary of work related to relay selection schemes.

Relay selection scheme	Category	High social intimacy	Good throughput performance	Ad hoc network	Low complexity
Intuitive method [9]	Category I	×	×	×	✓
Social-trust-based relay selection [6]	Category II	✓	×	×	✓
Physical-based relay selection [7]	Category II	×	✓	×	×
Hybrid social trust and physical relay selection [8], [10]	Category III	✓	✓	×	×
Social-physical relay reselection [11]	Category III	✓	✓	×	×
Our work	Category III	✓	✓	✓	✓

and a reselection approach [11] in the social-physical layers. In the following, we explain the distinctions among these related works.

In the intuitive method [9], a mobile relay moves to the midpoint location between the source and destination users for each link. This method can yield only a minor throughput gain, but it is widely applied in practice due to its low complexity. Social-trust-based relay selection [6] and physical-based relay selection [7], are extreme methods that consider either only social intimacy or only throughput for optimization. Consequently, their practicality is not high because of the excessive relay selection time. On the basis of [6] and [7], some researchers have comprehensively considered the interactions between social trust and user transmission distance to propose hybrid schemes [8], [10] and a relay reselection scheme [11]. Unfortunately, these methods are applicable only for cellular networks and the time cost of relay selection is prohibitive. In contrast to the existing works described above, our work focuses on social-physical ad hoc networks, aiming to achieve optimal throughput performance with high social intimacy and low complexity.

B. USER COOPERATIVE MOBILITY APPROACH

Grossglauser and Tse [14] first theoretically proved that user mobility behavior can be exploited to dramatically enhance the system throughput through path diversity. Subsequently, Baron *et al.* [15] demonstrated that the random mobility of portable devices can be viewed as providing opportunistic access to data that can effectively overcome base station constraints and increase throughput. Later, Murase [16] and Chaintreau *et al.* [17] showed that cooperative user mobility can reduce the resource consumption of service providers and effectively increase throughput. Thus, it can be effective to design an efficient algorithm based on human mobility paths to improve throughput at a low resource cost.

Fig. 1 depicts the application scenario for user cooperative mobility. We note that some fixed users on the city's periphery might experience a low transmission rate and poor throughput performance due to their distance from the nearest AP. Meanwhile, for work or business reasons, people close to an AP may move toward the edge of the city. These mobile users are able to carry data traffic and act as relays forwarding data to fixed users. Considering the signal-to-interference-plus-noise ratios (SINRs) between all users, it is worth addressing the issue of how to move these mobile users to the optimum positions.

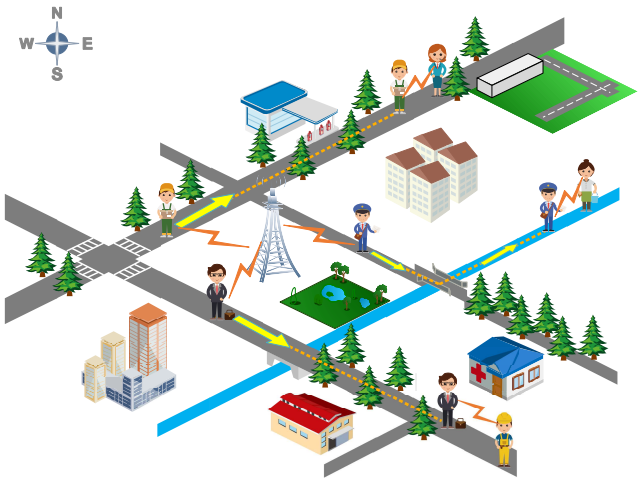

FIGURE 1. Application scenario of user cooperative mobility.

Miyata *et al.* [18] introduced an algorithm for selecting the optimal AP based on user mobility to maximize throughput. Luo and Murase [19] experimentally verified the system throughput gain for a single mobile user at the optimal location and validated the range of throughput variation under the capture effect. In addition, Okumura and Murase [20] proposed direct and indirect methods of analyzing the throughput performance of multiple networks in the presence of link bottlenecks. In our previous work [12], [13], we proposed an interaction position game and an efficient maximum throughput for optimal position (MTOP) algorithm to improve throughput and reduce complexity, respectively. However, a relevant practical algorithm for a multiuser cooperative mobility scheme in a physical-social network has not previously been investigated due to the complex transmission strategies and real-time requirements involved.

In summary, few researchers have comprehensively studied the challenge of pursuing effective collaboration to maximize throughput in social-physical ad hoc networks. Moreover, no appropriate strategy has been proposed and adopted to improve the system throughput of social networks through multiuser cooperative mobility, i.e., to maximize throughput with high intimacy and a low time cost for relay selection.

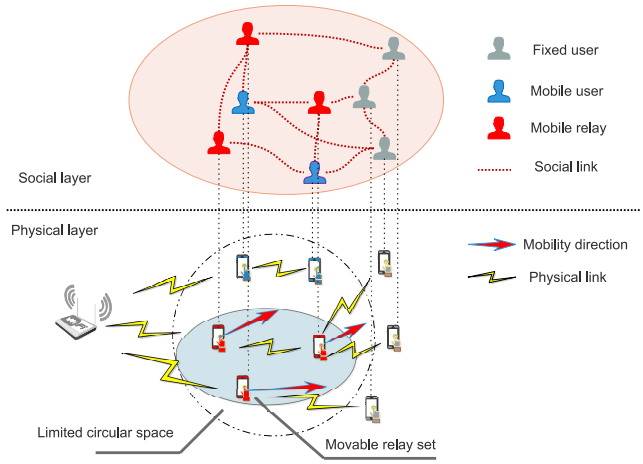

FIGURE 2. A social-physical dual-layer model based on multiuser cooperative mobility in an ad hoc network.

III. SYSTEM MODEL

In this section, we construct a social-physical dual-layer model and then analyze the channel model and interference.

A. A SOCIAL-PHYSICAL DUAL-LAYER MODEL BASED ON MULTIUSER COOPERATIVE MOBILITY IN AN AD HOC NETWORK

As shown in Fig. 2, we consider a multiuser cooperative mobility setting consisting of two layers, social and physical, deployed in an ad hoc network. In the physical layer, the data flows between the AP and fixed user devices (FUDs) pass through relay user devices (RUDs) via D2D communication, for which the RUDs are selected from among the mobile user devices (MUDs). For ease of notation, we define $\mathcal{H} = \{1, 2, \ldots, |H|\}$ as the user set that comprises both the FUDs $\mathcal{F} = \{f_i | 1 \le i \le |F|, i \in \mathbb{N}^+\}$ and the MUDs $\mathcal{M} = \{m_i | 1 \le i \le |M|, i \in \mathbb{N}^+\}$, where $|F| + |M| = |H|$. Meanwhile, the MUDs include both RUDs and nonrelay user devices; the former are denoted by $\widehat{\mathcal{R}} = \{\widehat{r}_i | 0 \le i \le |\widehat{R}|, i \in \mathbb{N}\}$ and the latter are represented by $\widetilde{\mathcal{R}} = \{\widetilde{r}_i | 0 \le i \le |\widetilde{R}|, i \in \mathbb{N}\}$, where $\mathcal{M} = \widehat{\mathcal{R}} \cup \widetilde{\mathcal{R}}$ and $|M| = |\widehat{R}| + |\widetilde{R}|$. Given user privacy concerns, the number of relay nodes requested by fixed users should be as small as possible to ensure data integrity and prevent privacy disclosure. To this end, we assume D2D pairs consisting of only one RUD and one FUD, i.e., $|F| = |\widehat{R}|$. The mobility area of the MUDs is a limited circular area, with a maximum radius of L.

To facilitate the analysis of system throughput, we consider the uplink data sent by both the FUDs and MUDs to the AP while all links are saturated as the basis for the throughput calculation. Based on this consideration, the system throughput is defined as the data rate per unit time of the entire D2D communication system, i.e., the amount of data received by the AP per unit time is equal to the harmonic mean transmission rate of all users [12]. Therefore, the objective of optimal relay selection and multiuser cooperative mobility for enhancing throughput can be characterized as maximizing the effective transmission time and SINR by considering mutual interference.

Additionally, each device can be mapped from the physical and social layers and connected to form a social network through social links. In the actual social layer, people interact through human habits, speech, and social ties. Here, the existence of each social link is determined on the basis of intimacy, which is an objective factor for judging the degree of likelihood of interaction between persons. To represent the detailed information on the intimacy among users, we leverage a social graph, defined as $\boldsymbol{G}_s = \{\mathcal{H}, \mathcal{S}\}$, where $\mathcal{S}$ represents the intimacy values. Specifically, we introduce an intimacy matrix $\mathcal{S} = (\boldsymbol{S}_1^T, \boldsymbol{S}_2^T, \ldots, \boldsymbol{S}_{|H|}^T) \in \mathbb{R}^{|H| \times |H|}$, where each row vector has the form $\boldsymbol{S}_i = (s_{i,1}, s_{i,2}, \ldots, s_{i,|H|}) \in \mathbb{R}^{1 \times |H|}$, $\forall i \in \{1, 2, \ldots, |H|\}$, with $s_{i,j}$ denoting the social trust value between user $i \in \mathcal{H}$ and another user $j \in \mathcal{H} \backslash \{i\}$. Here, $s_{i,j}$ is defined as

$$s_{i,j} = \begin{cases} (0,1], & \text{if } i \text{ and } j \text{ have social trust,} \\ 0, & \text{otherwise,} \end{cases} \tag{1}$$

where $s_{i,i} \equiv 1$ represents that a user completely trusts him- or herself. In reality, a reliable social relationship can be established only if the intimacy reaches a certain value. In other words, if $s_{i,j}$ is larger than a predefined threshold $\bar{s}$, then a stable social connection link can be established between the two corresponding users.

The application scenario for this model is briefly described as follows. Due to the distance from the AP or poor channel conditions, the transmission performance of many FUDs may be low. Particularly, such lower-rate nodes can seriously affect the system throughput according to performance anomaly theory [21], making it challenging to meet users' typical QoS requirements. Meanwhile, for work or travel reasons, some MUDs may need to move closer to the locations of FUDs. Consequently, these FUDs can ask some of their friends, i.e., MUDs that are friendly to them, to act as relays to transfer data traffic via D2D technology. In line with a common trend in many previous system control mechanisms [22]–[24], to enable accessible analysis and exploration of the system performance limits while gaining useful insights, we hypothesize that there exists a virtual controller in the AP that can control the actions of the RUDs and track the location information of each user. This controller is capable of running the proposed relay selection scheme and mobility algorithms. In addition, a summary of the intimacy information between users will also be provided to this controller to support overall decision-making.

It is well known that the signal interference between users can seriously reduce throughput performance and channel utilization. A promising way out of this gridlock is successive interference cancellation (SIC) [25], which enables the decoding of collided or superposed signals due to interference. Specifically, in the SIC mechanism, the signal can be successfully decoded as long as the SINR of the receiving user is above a certain threshold. In our model, the

SIC technique is deployed to combat conflicts arising in multipacket reception among different users. Additionally, the instantaneous channel state information (CSI) of the users is unknown to each user, but we assume the statistics of the users' channel gains can be obtained [26]. Therefore, the channel gain can be calculated, and the CSI is assumed to be known at the D2D transmitter. Each of the user devices is equipped with a single omnidirectional antenna.

In general, consideration of dynamic elements, including locations and social states of users, is crucial for ensuring the reliability of such dual-layer network. Therefore, solutions that focus exclusively on network throughput are not always aligned with high reliability, which, as mentioned above, is critical for the robustness and operational stability of ad hoc networks. A reliability parameter is defined as being equal to the Cartesian product of the social intimacy and the probability of successful transmission. Specifically, we characterize the following features to formulate the optimization problem:

- *Relay Selection Scheme:* RUDs are selected from among MUDs on the basis of high social intimacy and a low selection time. In other words, the optimal relay requires the shortest time consumption for selection while guaranteeing the validity of the social link.
- *Multiuser Cooperative Mobility Strategy:* The best throughput performance is achieved through the joint mobility of the mobile RUDs when the interference is minimized and the SINR is maximized.
- *Optimization Constraints:* The optimization problem should be constrained in three dimensions, namely, the existence of a social link (high intimacy), the existence of a physical link (high SINR) and the link of reliability.

Since the data stream is saturated, frame conflicts have less impact on the results according to the definition of the harmonic mean throughput and the SIC decoding mechanism. From an operational standpoint, in this paper, we are not concerned with the time assignment MAC frames or multipacket allocation; instead, we focus only on the selection and placement of the RUDs and on the interference among users. Additionally, this model considers only the dynamic changes in throughput before and after the relays' movement and ignores the data loss due to mobility, i.e., the time consumed is assumed to be short enough that the impact of mobility speed on the final throughput is negligible.

B. CHANNEL MODEL AND INTERFERENCE ANALYSIS

Given that the application scenario of interest will mainly arise in a plaza, park or other large meeting place, the wireless model used is the independent Rayleigh fading model. Under the assumption that the instantaneous channel gain $\boldsymbol{H}$ includes the Rayleigh channel fading coefficient, the received signal can be expressed as

$$\boldsymbol{Y} = P_r \boldsymbol{H}\boldsymbol{X} + n_0 \tag{2}$$

where $\boldsymbol{X}$ is the transmitted signal, P_r is the received power, and n_0 is additive white Gaussian noise (AWGN) following a Gaussian distribution $\mathcal{N}(0, N_0)$. The received power P_r is given by

$$P_r = P_t K d_r^{-\alpha} \tag{3}$$

where P_t denotes the received power; K is the shadowing constant, which can be calculated from the CSI statistics; d_r denotes the distance between the transmitter and the receiver; and α represents the path-loss index.

In this case, the envelope of the received signal $\boldsymbol{Y}$ will be Rayleigh distributed with the following probability density function (PDF):

$$f(y) = \frac{2y}{\Omega} \exp\left(-\frac{y^2}{\Omega}\right), y \geq 0 \tag{4}$$

where Ω is the average received power determined by the path-loss and shadowing effects. Hence, the received power P_r will be exponentially distributed with mean Ω, where $\Omega = \mathbb{E}(P_r)$. According to (2)-(4), the signal received at RUD $\widehat{r_i}$, $\widehat{r_i} \in \widehat{\mathcal{R}}$, is then given by

$$\begin{aligned} y_{\widehat{r_i}} = {} & H_{\mathrm{AP},\widehat{r_i}} \sqrt{P_{\mathrm{AP}} K d_{\mathrm{AP},\widehat{r_i}}^{-\alpha}} x_{\mathrm{AP}} \\ & + H_{m_j,\widehat{r_i}} \sqrt{P_{m_j} K d_{m_j,\widehat{r_i}}^{-\alpha}} x_{m_j} + n_0 \end{aligned} \tag{5}$$

where $H_{\mathrm{AP},\widehat{r_i}}$ denotes the channel fading coefficient from the AP to RUD $\widehat{r_i}$; P_{AP} is the transmission power of the AP; $H_{\mathrm{AP},\widehat{r_i}}$ is the Euclidean distance between the AP and RUD $\widehat{r_i}$; and x_{AP} is the signal from the AP with unit power. In particular, $H_{m_j,\widehat{r_i}} \sqrt{P_{m_j} K d_{m_j,\widehat{r_i}}^{-\alpha}} x_{m_j}$ represents the interference signal from m_j to $\widehat{r_i}$, where $m_j \in \widetilde{\mathcal{R}} \cup \widehat{\mathcal{R}} \backslash \{\widehat{r_i}\}$. Additionally, the received SINR at RUD $\widehat{r_i}$ can be expressed as

$$\gamma_{\mathrm{AP},\widehat{r_i}} = \frac{\left|H_{\mathrm{AP},\widehat{r_i}}\right|^2 P_{\mathrm{AP}} K d_{\mathrm{AP},\widehat{r_i}}^{-\alpha}}{\sum_{m_j \in \widetilde{\mathcal{R}} \cup \widehat{\mathcal{R}} \backslash \{\widehat{r_i}\}} \left|H_{m_j,\widehat{r_i}}\right|^2 P_{m_j} K d_{m_j,\widehat{r_i}}^{-\alpha} + n_0} \tag{6}$$

Similar to (5), the signal received at FUD f_i, $f_i \in \mathcal{F}$, is given by

$$\begin{aligned} y_{f_i} = {} & H_{\widehat{r_i},f_i} \sqrt{P_{\widehat{r_i}} K d_{\widehat{r_i},f_i}^{-\alpha}} x_{\widehat{r_i}} \\ & + H_{m_j,\widehat{r_i}} \sqrt{P_{m_j} K d_{m_j,\widehat{r_i}}^{-\alpha}} x_{m_j} + n_0 \end{aligned} \tag{7}$$

Accordingly, for the received SINR at FUD f_i, we have

$$\gamma_{\widehat{r_i},f_i} = \frac{\left|H_{\widehat{r_i},f_i}\right|^2 P_{\widehat{r_i}} K d_{\widehat{r_i},f_i}^{-\alpha}}{\sum_{m_j \in \widetilde{\mathcal{R}} \cup \widehat{\mathcal{R}} \backslash \{\widehat{r_i}\}} \left|H_{m_j,f_i}\right|^2 P_{m_j} K d_{m_j,f_i}^{-\alpha} + n_0} \tag{8}$$

In accordance with the SIC decoding mechanism, the SINR at any D2D receiver, including both RUD $\widehat{r_i}$ and FUD f_i, should be greater than $\overline{\gamma}$, which is the threshold for allowing the signal to be decoded correctly. In the next section, we consider these constraints regarding the social trust, physical SINR, and reliability to formulate an optimization problem.

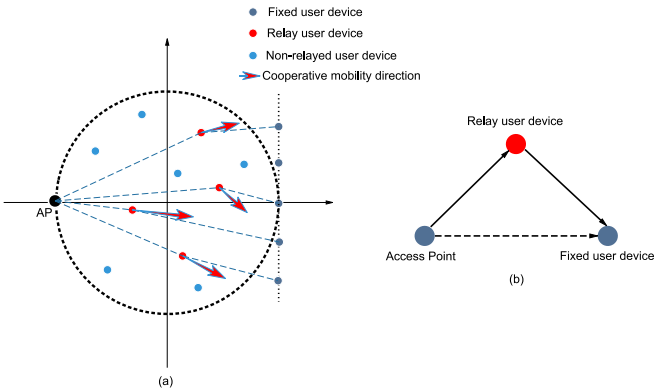

FIGURE 3. Mathematical model. (a) Data transmission topology model; (b) Illustration of amplify-and-forward (AF) relaying mode.

IV. RELAY SELECTION WITH MULTIUSER COOPERATIVE MOBILITY FOR THROUGHPUT MAXIMIZATION UNDER LINK RELIABILITY

In this section, we formulate the problem of maximizing the effective system throughput based on an optimal relay selection scheme and an optimal multiuser cooperative mobility strategy.

Fig. 3 shows the mathematical model describing the transmission topology and the amplify-and-forward (AF) relaying mode. Let $u_{\widehat{r}_i}$ and u_{f_i} denote the position coordinates of an arbitrary RUD $\widehat{r}_i$ and FUD f_i, respectively, where $u_{\widehat{r}_i}$ is treated as a variable and u_{f_i} is a constant. The distance between $\widehat{r}_i$ and f_i is expressed as $D_{\widehat{r}_i,f_i} = \|u_{\widehat{r}_i} - u_{f_i}\|$, which can be treated as a function of the variable $u_{\widehat{r}_i} \in \boldsymbol{U}$, where $\boldsymbol{U}$ is the set of position coordinates of the RUDs. Furthermore, we define the set of the distances between the RUDs and other users as $\boldsymbol{D} \triangleq \{(D_{\mathrm{AP},\widehat{r}_i}, D_{\widehat{r}_i,f_i}, D_{\widehat{r}_i,m_j}) | \widehat{r}_i \in \widehat{\mathcal{R}}, f_i \in \mathcal{F}, m_j \in \widetilde{\mathcal{R}} \cup \widehat{\mathcal{R}} \backslash \{\widehat{r}_i\}\}$. Once the distance set $\boldsymbol{D}$ has been calculated, the set of RUD position coordinates $\boldsymbol{U}$ is also uniquely determined. Therefore, in the following analysis, we simply use the distance set $\boldsymbol{D}$ to represent the RUD position coordinates $\boldsymbol{U}$ for brevity. To better represent the selection of RUDs from among the MUDs, we introduce an indicator function $\omega(m_i) \in \boldsymbol{\Omega}$ defined on the set $\mathcal{M}$, $m_i \in \mathcal{M}$:

$$\omega(m_i) = \begin{cases} 1, & \text{if } m_i = \widehat{r}_i, \\ 0, & \text{if } m_i = \widetilde{r}_i. \end{cases} \tag{9}$$

where $\boldsymbol{\Omega}$ is the set of indicator function values. In addition, we give a detailed lists of the notations for the main sets and parameters in Table 2.

According to [27], the AF relay mode has a greater array gain and a lower cost and complexity than the decode-and-forward (DF) mode for the same diversity gain. Here, to ensure high practicability, we adopt the AF mode to achieve cooperative diversity in our system model. Additionally, we assume that the transmission power P_{AP} from AP to each RUD is the same and that all nodes also have the same transmission power P_0 due to their identical antenna gain performance and use of the same transmission protocol,

TABLE 2. List of main sets and parameters.

Notations	Descriptions
$\mathcal{F}$	The set of fixed user devices (FUDs)
$\mathcal{M}$	The set of mobile user devices (MUDs)
$\widehat{\mathcal{R}}$	The set of relay user devices (RUDs)
$\mathcal{S}$	The set of intimacy values between users
$\boldsymbol{U}$	The set of position coordinates of the RUDs
$\boldsymbol{D}$	The set of distances between the RUDs and other users
$\boldsymbol{\Omega}$	The set of indicator function values
$s_{i,j}$	The social trust value between user $i \in \mathcal{H}$ and $j \in \mathcal{H} \backslash \{i\}$
T	The random variable of contact durations
R_{eff}	The effective data transmission rate
T_{eff}	The effective transmission time
p_r	The probability of successful transmission within T_{eff}
p	The link reliability
Th_{sys}	The system throughput

where $P_0 = P_{\widehat{r}_i} = P_{m_j}$. Hence, the achievable data rate pertaining to transmission from FUD $f_i \in \mathcal{F}$ in the AF mode is given by

$$\gamma_{\mathrm{AP},f_i} = \frac{\gamma_{\mathrm{AP},\widehat{r}_i}\gamma_{\widehat{r}_i,f_i}}{\gamma_{\mathrm{AP},\widehat{r}_i} + \gamma_{\widehat{r}_i,f_i} + 1} \tag{10}$$

Then, the maximum achievable end-to-end rate can be derived as

$$R_{\mathrm{AP},f_i} = \frac{1}{2}\mathscr{B}\log_2\left(1 + \frac{\gamma_{\mathrm{AP},\widehat{r}_i}\gamma_{\widehat{r}_i,f_i}}{\gamma_{\mathrm{AP},\widehat{r}_i} + \gamma_{\widehat{r}_i,f_i} + 1}\right) \tag{11}$$

where $\mathscr{B}$ is the normalized bandwidth. By substituting (6) and (8) into (11), R_{AP,f_i} can be rewritten as

$$\begin{aligned} R_{\mathrm{AP},f_i}(\boldsymbol{D}) &= \frac{1}{2}\log_2\left(\frac{1+\frac{P_{\mathrm{AP}}}{P_0}G_{\mathrm{AP},\widehat{r}_i}G_{\widehat{r}_i,f_i}\{D_{\mathrm{AP},\widehat{r}_i}D_{\widehat{r}_i,f_i}\}^{-\alpha}}{\phi 1 G_{\widehat{r}_i,f_i}D_{\widehat{r}_i,f_i}^{-\alpha} + \phi 2\frac{P_{\mathrm{AP}}}{P_0}G_{\mathrm{AP},\widehat{r}_i}D_{\mathrm{AP},\widehat{r}_i}^{-\alpha} + \phi 1\phi 2}\right) \\ \phi 1 &\triangleq \sum_{m_j \in \widetilde{\mathcal{R}} \cup \widehat{\mathcal{R}} \backslash \{\widehat{r}_i\}} G_{m_j,\widehat{r}_i}D_{\widehat{r}_i,f_i}^{-\alpha} + \frac{n_0}{P_0} \\ \phi 2 &\triangleq \sum_{m_j \in \widetilde{\mathcal{R}} \cup \widehat{\mathcal{R}} \backslash \{\widehat{r}_i\}} G_{m_j,f_i}D_{m_j,f_i}^{-\alpha} + \frac{n_0}{P_0} \end{aligned} \tag{12}$$

where $G_{\mathrm{AP},\widehat{r}_i} = K|H_{\mathrm{AP},\widehat{r}_i}|^2$, $G_{\widehat{r}_i,f_i} = K|H_{\widehat{r}_i,f_i}|^2$, $G_{m_j,\widehat{r}_i} = K|H_{m_j,\widehat{r}_i}|^2$ and $G_{m_j,f_i} = K|H_{m_j,f_i}|^2$ denote the channel gains among the AP, FUD f_i, RUD $\widehat{r}_i$ and MUD m_j. Here, the information on the relevant channel gain and CSI can be obtained from feedback on each link. Note that, the channel gains follow exponential distributions [28]. Specifically, $G_{\mathrm{AP},\widehat{r}_i}$ and $G_{m_j,\widehat{r}_i}$ obey exponential distributions with the same parameter $\frac{1}{\lambda}$, i.e., $G_{\mathrm{AP},\widehat{r}_i} \sim \mathrm{Exp}(\lambda)$, $G_{m_j,\widehat{r}_i} \sim \mathrm{Exp}(\lambda)$. Likewise, $G_{\widehat{r}_i,f_i}$ and G_{m_j,f_i} also follow exponential distributions with the same parameter $\frac{1}{\eta}$, i.e., $G_{\widehat{r}_i,f_i} \sim \mathrm{Exp}(\eta)$ and $G_{m_j,f_i} \sim \mathrm{Exp}(\eta)$. Therefore, the PDFs of these channel gains can be expressed as

$$f_{G_{\mathrm{AP},\widehat{r}_i}}(x) = f_{G_{m_j,\widehat{r}_i}}(x) = \frac{1}{\lambda}e^{-\frac{x}{\lambda}} \tag{13}$$

$$f_{G_{\widehat{r}_i,f_i}}(x) = f_{G_{m_j,f_i}}(x) = \frac{1}{\eta}e^{-\frac{x}{\eta}} \tag{14}$$

As mentioned in the section introducing the system model, the requirements in the relay selection process are to determine the cooperative gain and ensure the reliability of the social-physical dual-layer links. Let T denote the random variable representing the contact durations in a time slot, which follows a Gamma distribution [11], $T \sim Gamma(\mu, \rho)$. The PDF of T can be expressed as

$$f(X_T) = \frac{x_T^{(\mu-1)} \exp\left(-\frac{x_T}{\rho}\right)}{\Gamma(\mu)\rho^{\mu}} \tag{15}$$

Considering the selection time, we have the following effective transmission time:

$$\begin{aligned} T_{eff}(\boldsymbol{\Omega}) &= T - \sum_{m_i \in \mathcal{M}} \tau_{m_i}(\boldsymbol{\Omega}) \\ \tau_{m_i}(\boldsymbol{\Omega}) &= \tau_{m_i}\boldsymbol{\Omega}(m_i) \end{aligned} \tag{16}$$

where τ_{m_i} represents the time cost of relay selection, including both the detection time and the duration of algorithm execution. Specifically, τ_{m_i} follows the uniform distribution $\tau_{m_i} \sim U(0, T)$ [29]. Thus, we can obtain the cumulative distribution function (CDF) of the effective transmission time T_{eff} as

$$F_{T_{eff}}(t, \boldsymbol{\Omega}) = \int_0^{+\infty} \int_{X_T - t}^{X_T} \frac{x_T^{(\mu-2)} \exp\left(-\frac{x_T}{\rho}\right)}{\Gamma(\mu)\rho^{\mu}} d_{\tau_{m_i}} dX_T \tag{17}$$

Accordingly, we can obtain the PDF of T_{eff} as $f_{T_{eff}}(t) = F'_{T_{eff}}(t, \boldsymbol{\Omega})$. The expected effective transmission time can be calculated as $\mathbb{E}[T_{eff}] = \int_0^{+\infty} t f_{T_{eff}}(t) dt$. The effective data rate for transmission, R_{eff}, can be expressed as

$$\begin{aligned} R_{eff}(\boldsymbol{\Omega}, \boldsymbol{D}) &= R_{\mathrm{AP},f_i}(\boldsymbol{D}) \cdot T_{eff}(\boldsymbol{\Omega}) \\ &= R_{\mathrm{AP},f_i}(\boldsymbol{D}) \int_0^{+\infty} t F'_{T_{eff}}(t, \boldsymbol{\Omega}) dt \end{aligned} \tag{18}$$

Notably, the throughput Th_{sys} is the reciprocal of the harmonic mean in the case that links are all saturated, which is given by

$$Th_{sys} = \frac{|F|}{\sum_{i=1}^{|F|} \frac{1}{R_{eff}(\boldsymbol{\Omega}, \boldsymbol{D})}} \tag{19}$$

Additionally, to guarantee reliability under social-physical dual-layer model, we assume that the packet size required to be transmitted is Z; then, the probability $p_r(\boldsymbol{\Omega}, \boldsymbol{D})$ of successful data transmission within T_{eff} is expressed as

$$\begin{aligned} p_r(\boldsymbol{\Omega}, \boldsymbol{D}) &= \Pr\left\{ R_{AP,f_i}(\boldsymbol{D}) \geq \frac{Z}{T_{eff}} \right\} \\ &= \Pr\left\{ \frac{\frac{P_{\mathrm{AP}} G_{\mathrm{AP},\widehat{r}_i} G_{\widehat{r}_i,f_i} \left\{ D_{\mathrm{AP},\widehat{r}_i} D_{\widehat{r}_i,f_i} \right\}^{-\alpha}}{\phi 1 \phi 2 P_0}}{\frac{P_{\mathrm{AP}} G_{\mathrm{AP},\widehat{r}_i} D_{\mathrm{AP},\widehat{r}_i}^{-\alpha}}{P_0 \phi 1} + \frac{G_{\widehat{r}_i,f_i} D_{\widehat{r}_i,f_i}^{-\alpha}}{\phi 2} + 1} \geq 2^{\frac{2Z}{WT_{eff}}} - 1 \right\} \end{aligned} \tag{20}$$

Evidently, the success probability $p_r(\boldsymbol{\Omega}, \boldsymbol{D})$ is related to the variables $G_{\mathrm{AP},\widehat{r}_i}$ and $G_{\widehat{r}_i,f_i}$. We introduce the following theorem to verify the properties of this probability and calculate $p_r(\boldsymbol{\Omega}, \boldsymbol{D})$ based on Eq. (13), Eq. (14), and Eq. (20).

Theorem 1: If the variables A and B both obey the independent exponential distribution with the parameters $\zeta_A = \lambda$ and $\zeta_B = \eta$, respectively, then the CDF of $Y = k_1 k_2 AB/(k_1 A + k_2 B + 1)$, with $k_1, k_2 > 0$, can be derived as

$$F_Y(y) = 1 - \frac{k_1 e^{-\frac{\lambda y}{k_1 k_2 - k_1 y}} (k_2 - y)}{k_1 k_2 \eta - k_1 \eta y + k_2 \lambda y} \tag{21}$$

Proof: Since A and B are continuous random variables and independently follow exponential distributions, we have

$$\begin{aligned} F_Y(y) &= P\{Y \leq y\} = P\{k_1 k_2 AB/(k_1 A + k_2 B + 1) \leq y\} \\ &= \int_0^{+\infty} \int_0^{\frac{y(k_2 b+1)}{k_1 k_2 b - k_1 y}} \lambda e^{-\lambda a} \eta e^{-\eta b} da db \\ &= 1 - \frac{k_1 e^{-\frac{\lambda y}{k_1 k_2 - k_1 y}} (k_2 - y)}{k_1 k_2 \eta - k_1 \eta y + k_2 \lambda y} \end{aligned} \tag{22}$$

■

Let $k_1 = \frac{P_{\mathrm{AP}} D_{\mathrm{AP},\widehat{r}_i}^{-\alpha}}{P_0 \phi 1}$ and $k_2 = \frac{D_{\widehat{r}_i,f_i}^{-\alpha}}{\phi 2}$; then, the CDF of Y is given by

$$\begin{aligned} F_{R_{AP,f_i}(\boldsymbol{D})}\left(R_{AP,f_i}(\boldsymbol{D})\right) &= \Pr\left\{ Y \leq 2^{2R_{AP,f_i}(\boldsymbol{D})} - 1 \right\} \\ &= F_Y\left(2^{2R_{AP,f_i}(\boldsymbol{D})} - 1\right) \end{aligned} \tag{23}$$

Therefore, we have

$$\begin{aligned} p_r(\boldsymbol{\Omega}, \boldsymbol{D}) &= \Pr\left(R_{AP,f_i}(\boldsymbol{D}) \geq \frac{Z}{T - \sum_{i \in \mathcal{M}} \tau_i(\boldsymbol{\Omega})} \right) \\ &= 1 - F_{R_{AP,f_i}(\boldsymbol{D})}\left(\frac{Z}{T - \sum_{i \in \mathcal{M}} \tau_i(\boldsymbol{\Omega})} \right) \\ &= 1 - F_Y\left(2^{\frac{Z}{T - \sum_{i \in \mathcal{M}} \tau_i(V)}} - 1 \right) \end{aligned} \tag{24}$$

Then, by substituting (24) into (21), the probability $p_r(\boldsymbol{\Omega}, \boldsymbol{D})$ of successful end-to-end data transmission can be calculated as

$$\begin{aligned} p_r(\boldsymbol{\Omega}, \boldsymbol{D}) &= \frac{k_1 \exp\left(-\frac{\lambda}{\frac{k_1 k_2 (T - \sum_{i \in \mathcal{M}} \tau_i(\boldsymbol{\Omega}))}{Z} - k_1} \right)}{k_1 k_2 \eta + (k_2 \lambda - k_1 \eta)\left(2^{\frac{Z}{T - \sum_{i \in \mathcal{M}} \tau_i(\boldsymbol{\Omega})}} - 1 \right)} \\ &\quad \times \left(k_2 - 2^{\frac{Z}{T - \sum_{i \in \mathcal{M}} \tau_i(\boldsymbol{\Omega})}} - 1 \right), \\ k_1 &\triangleq \frac{P_{\mathrm{AP}} D_{\mathrm{AP},\widehat{r}_i}^{-\alpha}}{P_0 \phi 1}, \\ k_2 &\triangleq \frac{D_{\widehat{r}_i,f_i}^{-\alpha}}{\phi 2}. \end{aligned} \tag{25}$$

Consider that the RUDs are required not only to possess the intimacy and an SINR greater than given thresholds in the dual social-physical layers but also to ensure the reliability of the network; thus, the link reliability can be expressed as

$$p(\boldsymbol{\Omega}, \boldsymbol{D}) = p_r(\boldsymbol{\Omega}, \boldsymbol{D}) s_{i,j}(\boldsymbol{\Omega}) \tag{26}$$

where $s_{i,j}(\boldsymbol{\Omega})$ is the social intimacy after relay selection.

We note that the reliability is the Cartesian product of the transmission success probability and the social intimacy. Consequently, by summarizing (9) to (26), the optimal relay selection and multiuser cooperative mobility strategy to maximize the system throughput can be formulated as follows:

$$\begin{aligned}
\max_{\boldsymbol{\Omega},\boldsymbol{D}} \quad & \frac{|F|}{\sum_{i=1}^{|F|} \frac{1}{R_{eff,f_i}(\boldsymbol{\Omega},\boldsymbol{D})}} \\
\text{s.t.} \quad & s_{\widehat{r}_i,m_j}(\boldsymbol{\Omega}) \geq \overline{s}, \\
& s_{\widehat{r}_i,f_i}(\boldsymbol{\Omega}) \geq \overline{s}, \\
& p(\boldsymbol{\Omega},\boldsymbol{D}) \geq \overline{p}, \\
& \frac{\gamma_{\mathrm{AP},\widehat{r}_i}\gamma_{\widehat{r}_i,f_i}}{\gamma_{\mathrm{AP},\widehat{r}_i}+\gamma_{\widehat{r}_i,f_i}+1} \geq \overline{\gamma}, \\
& \gamma_{\widehat{r}_i,f_i} \geq \overline{\gamma}, \\
& \gamma_{\mathrm{AP},\widehat{r}_i} \geq \overline{\gamma}, \\
& D_{\widehat{r}_i,f_i} \leq 2L, \\
& D_{\widehat{r}_i,m_j} \leq 2L, \\
& \widehat{r}_i \in \widehat{\mathcal{R}}, f_i \in \mathcal{F}, m_j \in \widetilde{\mathcal{R}} \cup \widehat{\mathcal{R}} \backslash \{\widehat{r}_i\}.
\end{aligned} \tag{27}$$

where $\overline{p}$ is a reliability threshold that is predefined in accordance with the requirements of the real application scenario and satisfies $\overline{p} \in [0, 1]$. Both the objective function and constraints are nonconvex and nonlinear; that is, the problem can be interpreted as a nonconvex and nonlinear (NCNL) problem, which is a typical NP-hard problem. Although this problem can be solved through exhaustive search, the complexity of doing so is prohibitive due to the properties of NCNL problems. In practical applications, the controller execution algorithm's latency plays an essential role in determining the overall performance, mostly the relay selection time and user experience. Therefore, we propose a new method to address this issue in the next section.

V. RELAY SELECTION AND LINK INTERFERENCE DEGREE GRAPH (RS-LIDG) ALGORITHM

There are several available optimization packages, such as CVX for MATLAB and the Python Optimization Package, for solving convex optimization problems. However, an NCNL optimization problem cannot be solved to the global optimum with low computational complexity using traditional heuristic algorithms or optimization tools. Consequently, it is desirable to develop an effective and adaptable algorithm that can be deployed in actual ad hoc networks.

In this paper, the optimization problem given in Eq. (27) is decomposed into two subproblems, and the RS-LIDG algorithm is proposed to solve this problem completely. The proposed relay selection scheme based on the optimal stopping approach is proven to be efficient. Meanwhile, on the basis of a graph defined to represent the degrees of interference between physical links and Algorithm 1, it is demonstrated that the proposed multiuser cooperative mobility strategy can achieve the optimal throughput.

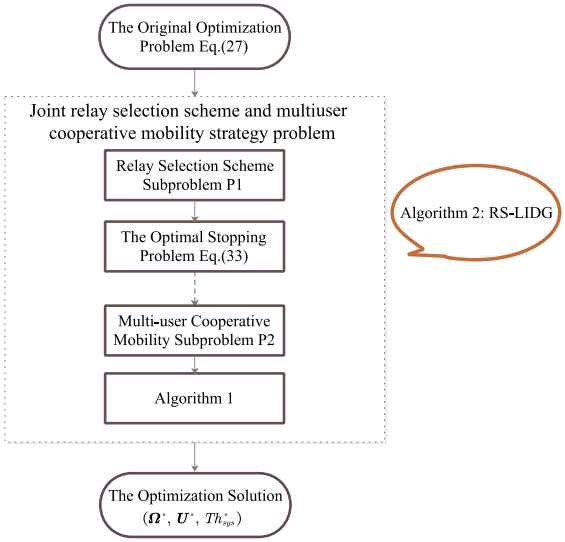

FIGURE 4. The proposed framework for solving the optimization problem given in Eq. (27).

The framework of our proposed RS-LIDG algorithm is shown in Figure 4.

A. RELAY SELECTION SCHEME

Based on (16) and (27), the goal of relay selection is to choose a sequence of actions such that the system will achieve the optimal throughput performance in terms of the maximal effective transmission time (minimal selection cost time) and sufficiently large intimacy. Accordingly, the relay selection subproblem can be expressed as

$$\begin{aligned}
(\mathbf{P1}): \quad & \max_{\boldsymbol{\Omega}} \ T_{eff}(\boldsymbol{\Omega}) \\
\text{s.t.} \quad & T_{eff}(\boldsymbol{\Omega}) = T - \sum_{m_i \in \mathcal{M}} \tau_{m_i} \boldsymbol{\Omega}(m_i), \\
& s_{\widehat{r}_i,m_j}(\boldsymbol{\Omega}) \geq \overline{s}, \\
& s_{\widehat{r}_i,f_i}(\boldsymbol{\Omega}) \geq \overline{s}, \\
& \widehat{r}_i \in \widehat{\mathcal{R}}, f_i \in \mathcal{F}, m_j \in \widetilde{\mathcal{R}} \cup \widehat{\mathcal{R}} \backslash \{\widehat{r}_i\}
\end{aligned} \tag{28}$$

Notably, for the selection of appropriate relays, it is required that the social intimacies between the RUDs, FUDs, and other MUDs (not relays) be greater than a predefined threshold, which depends on the specific scenario of interest. In this case, the optimal first step for the AP is to select viable relays to ensure stable social links, providing a solid foundation for effective and trustworthy peer-to-peer assistance in the multiuser cooperative mobility approach.

Then, the relay selection optimization problem defined in (28) can be cast as a finite-horizon optimal stopping problem, i.e., an optimal stopping policy can be set to maximize the expected reward by stopping in the optimal stopping phase. In fact, this scheme builds on the socially aware relay selection paradigm proposed in [6], in which the social tie structure is based on a cellular network and a time scheduling framework. Despite this similarity, we mainly focus on

relay resource segmentation and minimizing the time cost of selection through the ad hoc network's social-physical layers.

Suppose that the virtual controller observes two random sequences, consisting of relay detection time costs $\tau_{m_{(1)}}\boldsymbol{\Omega}(m_{(1)}), \tau_{m_{(2)}}\boldsymbol{\Omega}(m_{(2)}), \ldots,$ and communication durations $T_{(1)}, T_{(2)}, \ldots,$, through signal detection. Then, the controller must decide whether to stop after the detection of the k^{th} relay and achieve an effective transfer time T_{eff}^{k} or to continue to detect the next viable relay. It is possible that the controller might skip all potential MUDs without selecting any relays until all MUDs have been detected. In this case, direct communication would be established between the AP and the FUDs without any relays, for which $\tau_{m_{(0)}}\boldsymbol{\Omega}(m_{(0)}) = 0$ and $T_{eff}^{0} = T_{(0)}$. We first define the optimal stopping phase index as $k^* \in \mathcal{M}$, where $\sum_{k^*\in\mathcal{M}} |k^*| = |M|$ and $|k^*|$ denotes the number of stopping phase indices. The maximal effective transmission time, denoted by T_{eff}^{*}, satisfies the following:

$$\begin{aligned} T_{eff}^{*} &\overset{\text{def}}{=} \sup_{k\in\mathcal{M}}\Big[\mathbb{E}\Big(T_{eff}^{k}\Big)\Big] \\ k^* &\overset{\text{def}}{=} \arg\max_{k\in\mathcal{M}}\Big[\mathbb{E}\Big(T_{eff}^{j}\Big)\Big] \end{aligned} \tag{29}$$

According to optimal stopping theory [8], the effective transmission time T_{eff}^{k} can be defined as the instantaneous reward $T_{eff}^{k}[T, \tau_{m_{(k)}}\boldsymbol{\Omega}(m_{(k)})]$ when the controller decides to transmit after detecting the k^{th} relay. Therefore, we have

$$T_{eff}^{k}\big[T, \tau_{m_{(k)}}\boldsymbol{\Omega}\big(m_{(k)}\big)\big] = T - \sum_{m_k\in\mathcal{M}} \tau_{m_k}\boldsymbol{\Omega}(m_k) \tag{30}$$

Moreover, we use $\Phi_{eff}^{k}(T, \tau_{m_{(k)}}\boldsymbol{\Omega}(m_{(k)}))$ to denote the expected achievable reward for the system upon detecting the k^{th} relay. Since T and τ_{m_k} are mutually independent and follow gamma and uniform distributions, respectively, with PDFs $f_T(x)(\cdot)$ and $f_{\tau_{m_k}}(x)(\cdot)$, which are related to the indicator function, the expected achievable reward is given by

$$\begin{aligned} &\Phi_{eff}^{k}\big(T, \tau_{m_{(k)}}\boldsymbol{\Omega}\big(m_{(k)}\big)\big) \\ &\quad = \max\left\{\begin{array}{c} T_{eff}^{k}\big[T, \tau_{m_{(k)}}\boldsymbol{\Omega}\big(m_{(k)}\big)\big], \\ \mathbb{E}\Big[\Phi_{eff}^{k+1}\big(T, \tau_{m_{(k+1)}}\boldsymbol{\Omega}\big(m_{(k+1)}\big)\big)\Big] \end{array}\right\} \end{aligned} \tag{31}$$

where $\mathbb{E}[\Phi_{eff}^{k+1}(T, \tau_{m_{(k+1)}}\boldsymbol{\Omega}(m_{(k+1)}))]$ denotes the expected effective transmission time in the $(k+1)^{th}$ detection phase. This means that $\mathbb{E}[\Phi_{eff}^{k+1}(T, \tau_{m_{(k+1)}}\boldsymbol{\Omega}(m_{(k+1)}))]$ serves as the threshold for the controller to make its decision. Specifically, the AP compares these two values to determine whether to proceed beyond the k^{th} detection phase. If the instantaneous reward $T_{eff}^{k}[T, \tau_{m_{(k)}}\boldsymbol{\Omega}(m_{(k)})]$ is larger than this threshold, then the controller stops detecting and selects the current MUD as the final RUD. Otherwise, the detection process continues until no further potential MUD is detected. In this case, the reward threshold in the k^{th} phase is expressed as

$$\Xi_k^{*} = \mathbb{E}\Big[\Phi_{eff}^{k+1}\big(T, \tau_{m_{(k+1)}}\boldsymbol{\Omega}\big(m_{(k+1)}\big)\big)\Big] \tag{32}$$

Note that if the final phase is the $|M|^{th}$ phase ($k^* = |M|$), i.e., there are no more relays to be detected, then we set $\Xi_{|M|}^{*} = -\infty$ to represent that the controller terminates the detection process after the $|M|^{th}$ phase. Consequently, we can derive the optimal stopping policy for relay selection in the social-physical layers as described in Theorem 2 below.

Theorem 2: The optimal choice is for the controller to stop detection in phase k^* if the social-physical relay selection problem satisfies the following condition:

$$k^* = \min_{k\in\mathcal{M}}\Big\{k \geq 1 : T_{eff}^{k}\big[T, \tau_{m_{(k)}}\boldsymbol{\Omega}\big(m_{(k)}\big)\big] \geq \Xi_k^{*}\Big\} \tag{33}$$

where the thresholds $\{\Xi_k^{*}\}$ of the optimal stopping policy are given by

$$\begin{aligned} \Xi_{|M|}^{*} &= -\infty, \\ \Xi_{|M|-1}^{*} &= (\tau_{\max} - \tau_{\min}) \int_{T_{\min}}^{T_{\max}} \frac{t^{(\mu-1)} e^{\left(-\frac{t}{\rho}\right)}}{\Gamma(\mu)\rho^{\mu}} dt \\ &\quad - \sum |M| \int_{T_{\min}}^{T_{\max}} \int_{\tau_{\min}}^{\tau_{\max}} \tau \frac{t^{(\mu-1)} e^{\left(-\frac{t}{\rho}\right)}}{\Gamma(\mu)\rho^{\mu}} d\tau dt, \\ &\vdots \\ \Xi_k^{*} &= \big[\tau_{\max} + \big(\Xi_{k+1}^{*} - 1\big)\Xi_k - \Xi_{k+1}^{*}\tau_{\min}\big] \\ &\quad \times \int_{T_{\min}}^{T_{\max}} \frac{t^{(\mu-2)} e^{\left(-\frac{t}{\rho}\right)}}{\Gamma(\mu)\rho^{\mu}} dt \\ &\quad - \sum |k+1| \int_{T_{\min}}^{T_{\max}} \int_{\Xi_k}^{\tau_{\max}} \frac{t^{(\mu-2)} e^{\left(-\frac{t}{\rho}\right)}}{\Gamma(\mu)\rho^{\mu}} d\tau dt, \\ &\forall k = 0, 1, \ldots, |M| - 2 \end{aligned} \tag{34}$$

with $\Xi_k = \frac{(\Xi_{k+1} - \sum|k+1|)}{k} + (k+1)\tau$ and $\sum|k| = \sum_{i=1}^{|k|} \tau_{m_{(k)}}\boldsymbol{\Omega}(m_{(k)})$.

Proof: See the Appendix. ∎

Remark 1: The thresholds $\{\Xi_k^{*}\}_{k=1}^{|M|-2}$ can be interpreted as the maximal expected reward that the controller can find by seeking a better relay from phase $k+1$ to phase $|M|$ rather than performing data transmission after the k^{th} phase. Thus, the controller will compute the sequence of thresholds $\{\Xi_k^{*}\}_{k=1}^{|M|-2}$ in accordance with **Theorem 2** before relay signal detection. Once relay detection starts, the controller in the AP compares the instantaneous reward $T_{eff}^{k}[T, \tau_{m_{(k)}}\boldsymbol{\Omega}(m_{(k)})]$ against the expected threshold Ξ_k^{*}. If the threshold is greater than this instantaneous reward, then the controller continues to detect the next relay; otherwise, it terminates the detection process and decides to proceed to the multiuser cooperative mobility phase. In such a case, the indicator function $\boldsymbol{\Omega}(m_i)$ for relay selection can be obtained as

$$\begin{aligned} \boldsymbol{\Omega}(m_i) &= \Big(\mathcal{A}^T, \mathcal{B}^T\Big), \\ \mathcal{A}^{|\widehat{R}|\times 1} &\triangleq \Big(\mathbf{1}_{(0)}, \ldots, \mathbf{1}_{(k^*)}, \ldots, \mathbf{1}_{(|\widehat{R}|)}\Big)^T, \\ \mathcal{B}^{(|M|-|\widehat{R}|)\times 1} &\triangleq \big(\mathbf{0}, \ldots, \mathbf{0}_{(j)}, \ldots, \mathbf{0}\big)^T, \\ k^* &:= \arg\min_{k}\big(\Xi_k^{*}\big), j \in \mathcal{M} \setminus \big\{k^*\big\} \end{aligned} \tag{35}$$

where $\boldsymbol{\Omega}(m_i)$ indicates that each relay is selected in accordance with the optimal stopping policy, i.e., the previously described process of comparison against an expected threshold Ξ_k^* in the k^{th} phase needs to be repeated $|F|$ times until a sufficient number of relays are selected, and the label of each selected relay is k.

To summarize, our relay selection scheme can be described in two steps. The first step is to select feasible relays to ensure stable social links such that each link's intimacy is greater than a predefined threshold. In the second step, the relays with the longest effective transmission times are selected on the basis of the optimal stopping problem.

B. LINK INTERFERENCE DEGREE GRAPH

After relay selection, problem (27) is transformed into a relay-location-based optimization problem, in which the relay coordinates that maximize the throughput can be attained through multiuser cooperative mobility. Therefore, the optimization problem based on the RUD distance variables $\boldsymbol{D}$ can be expressed as

$$
\begin{aligned}
(\mathbf{P2}):\ \max_{\boldsymbol{D}}\ & \frac{|F|}{\sum_{i=1}^{|F|}\frac{1}{R_{eff,f_i}(\boldsymbol{D})}} \\
\text{s.t.}\ & p(\boldsymbol{D}) \geq \overline{p}, \\
& \frac{\gamma_{\mathrm{AP},\widehat{r}_i}\gamma_{\widehat{r}_i,f_i}}{\gamma_{\mathrm{AP},\widehat{r}_i}+\gamma_{\widehat{r}_i,f_i}+1} \geq \overline{\gamma}, \\
& \gamma_{\widehat{r}_i,f_i} \geq \overline{\gamma}, \\
& \gamma_{\mathrm{AP},\widehat{r}_i} \geq \overline{\gamma}, \\
& D_{\widehat{r}_i,f_i} \leq 2L, \\
& D_{\widehat{r}_i,m_j} \leq 2L, \\
& \widehat{r}_i \in \widehat{\mathcal{R}}, f_i \in \mathcal{F}, m_j \in \widetilde{\mathcal{R}} \cup \widehat{\mathcal{R}} \backslash \{\widehat{r}_i\}
\end{aligned} \tag{36}
$$

The goal of this problem can be characterized as choosing the optimal coordinates for the RUDs to achieve the highest transmission rate and throughput performance with limited distance and interference between nodes while satisfying all physical constraints and reliability requirements. Since **P2** is a nonconvex optimization problem, we would like to transform it into a convex problem using graph theory concepts. Therefore, we introduce the definition of the link interference degree graph. Within the limited circular space $\mathbb{C}$, the communication links established with the D2D technique in the ad hoc network can be represented by a physical graph $\boldsymbol{G}_p = (\mathcal{H}, E)$, where $\mathcal{H}$ is the set of all device nodes and edge $(u, v) \in E$ exists only if the SINR of the link between nodes u and v is no less than a threshold value $\overline{\gamma}$.

Definition 1 (Link Interference Degree Graph (LIDG)): Given a communication graph $\boldsymbol{G}_p = (\mathcal{H}, E)$, the corresponding LIDG $\boldsymbol{G}_{LIDG} = (\mathcal{V}, \mathcal{E})$ has the following properties:

- $\mathcal{V}$ and E are mutually contained and equal; that is, a vertex $v \in \mathcal{V}$ is introduced for each link $e \in E$ in $\boldsymbol{G}_p = (\mathcal{H}, E)$. A weighted edge $e \in \mathcal{E}$ is inserted between nodes $u, v \in \mathcal{V}$ that interfere with each other, where u and v correspond to links $e_1, e_2 \in E$ in the physical graph. Specifically, the weights of the edges represent the degrees of interference at the receiver nodes.
- $\boldsymbol{G}_{LIDG} = (\mathcal{V}, \mathcal{E})$ is a directed graph, and each directed edge $e_i = (u, v) \in \mathcal{E}$ is assigned a weight $W_{u,v}^i$, where $W_{u,v}^i \neq W_{v,u}^j$. This means that two vertices $e_i = (u, v)$ and $e_j = (v, u)$ in $\boldsymbol{G}_{LIDG} = (\mathcal{V}, \mathcal{E})$ generally do not have equal link interference degrees as a result of the channel states and fading coefficients.
- Each vertex $v \in \mathcal{V}$ has an incoming degree I_v and an outgoing degree O_v, where the incoming degree represents the level of interference of other nodes with that node and the outgoing degree represents its level of interference with other nodes. Node $v \in \mathcal{V}$ in $\boldsymbol{G}_{LIDG} = (\mathcal{V}, \mathcal{E})$ is feasible if and only if

$$
\frac{P_v^i}{n_0 + \sum_{\mathcal{V}\backslash\{v\}} I_v} \geq \overline{\gamma} \tag{37}
$$

where P_v^i is the received power, which depends on d_v, i.e., the geometric distance of this link in the communication graph $\boldsymbol{G}_p$.

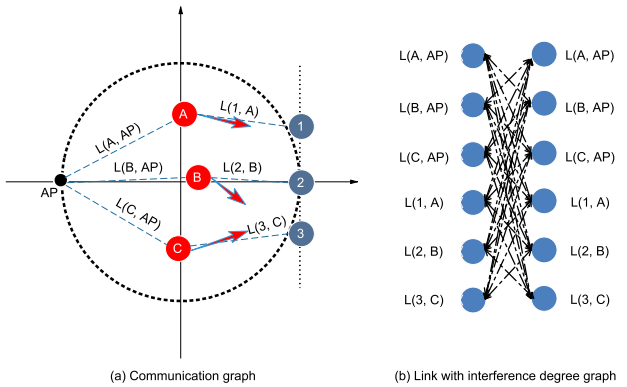

FIGURE 5. A specific illustration explains the definition and attributes of the LIDG: (a) Communication graph; (b) Link interference degree graph.

A specific illustration is given, as shown in Fig. 5, to better characterize the definition and attributes of the LIDG. In Fig. 5(a), the RUDs (nodes A, B and C) act as transmission intermediaries connecting the AP and the FUDs (nodes 1, 2 and 3), ultimately forming six communication links, L(A, AP), . . . , L(3, C). These links correspond to nodes in Fig. 5(b), and the weighted edges between these nodes are bidirectional, representing the corresponding degrees of interference. Specifically, $\boldsymbol{G}_{LIDG} = (\mathcal{V}, \mathcal{E})$ is a directed complete graph in which all edges are directed and two edges with opposite directions connect every pair of vertices. For an arbitrary pair of bidirectional edges $e_i = (u, v) \in \mathcal{E}$ and $e_j = (v, u) \in \mathcal{E}$, their weights $W_{u,v}^i$ and $W_{v,u}^j$ are generally not equal in value, that is, $W_{u,v}^i \neq W_{v,u}^j$. Therefore, the set of weights for these bidirectional edges forms a weight matrix

with zeros on the diagonal, $\Theta^{2|F|\times 2|F|}$, which is expressed as

$$\Theta = \begin{pmatrix} 0 & W^1_{2,1} & \cdots & W^1_{u,1} & \cdots & W^1_{2|F|-1,1} & W^1_{2|F|,1} \\ W^1_{1,2} & 0 & \cdots & W^2_{u,2} & \cdots & W^2_{2|F|-1,2} & W^2_{2|F|,2} \\ \cdots & \cdots & \cdots & \cdots & \cdots & \cdots & \cdots \\ W^i_{1,v} & W^i_{2,v} & \cdots & W^i_{u,v} & \cdots & W^i_{2|F|-1,v} & W^i_{2|F|,v} \\ \cdots & \cdots & \cdots & \cdots & \cdots & \cdots & \cdots \\ W^{2|F|-1}_{1,2|F|-1} & W^{2|F|-1}_{2,2|F|-1} & \cdots & \cdots & \cdots & 0 & W^{2|F|-1}_{2|F|,2|F|-1} \\ W^{2|F|}_{1,2|F|} & W^{2|F|}_{2,2|F|} & \cdots & W^{2|F|}_{u,2|F|} & \cdots & W^{2|F|}_{2|F|-1,2|F|} & 0 \end{pmatrix} \tag{38}$$

Furthermore, for any node $v \in \mathcal{V}$, the incoming degree I_v and the outgoing degree O_v are given by

$$I_v = \sum_{u=1}^{2|F|} W^i_{u,v} = \sum_n \Theta(m,n) \tag{39}$$

$$O_v = \sum_{u=1}^{2|F|} W^j_{v,u} = \sum_m \Theta(m,n) \tag{40}$$

According to (6) and (8), $W^i_{u,v}$ and $W^j_{v,u}$ can be expressed as

$$W^i_{u,v} = \left|H^i_{u,v}\right|^2 P^i_u K d^{-\alpha}_{u,v} \tag{41}$$

$$W^j_{v,u} = \left|H^j_{v,u}\right|^2 P^j_v K d^{-\alpha}_{v,u} \tag{42}$$

where $H^i_{u,v}$ is the channel fading coefficient from node u to node v; P^i_u is the transmission power of node u, $P^i_u = P_0 K d_u^{-\alpha}$; and $d_{u,v}$ denotes the distance between nodes u and v, $d_{u,v} = d_{v,u}$, i.e., the interference power of the transmitting node on link u with respect to the receiving node on link v in the physical graph $\boldsymbol{G}_p = (\mathcal{H}, E)$.

Theorem 3: A sufficient and necessary condition for achieving the maximum system throughput is to minimize the sum of the incoming and outgoing degrees for all nodes in $\boldsymbol{G}_{LIDG} = (\mathcal{V}, \mathcal{E})$. To this end, the following should be satisfied:

$$\max_{\boldsymbol{D}} \frac{|F|}{\sum_{i=1}^{|F|} \frac{1}{R_{eff\text{-}f_i}(\boldsymbol{D})}} \rightleftharpoons \min_{d_u, d_v, d_{u,v}} \sum_{\substack{u,\, v \in \mathcal{V} \\ i,\, j \in \mathcal{E}}} (I_v + I_o) \tag{43}$$

where d_u and d_v represent the geometric distances of links e_1 and e_2, respectively, that is, $d_u \sim e_1$ and $d_v \sim e_2$, for $e_1, e_2 \in E$ in the communication graph $\boldsymbol{G}_p$.

Proof: On the one hand, the maximum throughput of this ad hoc network is equivalent to the maximum transmission rate per unit time for adequacy. In other words, the transmission rate of the whole system is globally optimal for the locations of the relay nodes after mobility within the limited circular space $\mathbb{C}$. At this point, globally, the total SINR among nodes is maximized. Thus, with a known constant transmission power, the total interference among nodes is minimized. The minimization of the total interference implies the minimization of the sum of all nodes' incoming and outgoing degrees, which reflects the total level of interference in the system.

On the other hand, when the sum of the incoming and outgoing degrees of all nodes is minimized, the global interference level is minimized, which means that the SINR of this ad hoc network is maximized. The effective transmission rate of the nodes is also maximized, implying that the maximum throughput can be obtained at the locations after the relay nodes have moved. Hence, the necessity has been proven. ■

Remark 2: As mentioned, the objective function of this optimization problem is a nonconvex function, and therefore, **P2** is obviously a nonconvex optimization problem. According to **Theorem 3**, instead of maximizing the system throughput, the objective function can be recast to minimize the sum of the incoming and outgoing degrees of all nodes in $\boldsymbol{G}_{LIDG} = (\mathcal{V}, \mathcal{E})$. Thus, we obtain the following optimization problem:

$$\begin{aligned} (\mathbf{P3}): \min_{d_u, d_v, d_{u,v}} & \sum_{\substack{u,\, v \in \mathcal{V} \\ i,\, j \in \mathcal{E}}} (I_v + I_o) \\ \text{s.t. } & p_r\big(d_u, d_v, d_{u,v}\big) s_{u,v}(\boldsymbol{\Omega}) \geq \overline{p}, \\ & \frac{P_0 K d_u^{-\alpha} d_v^{-\alpha}}{d_u^{-\alpha}[I_v + n_0] + d_v^{-\alpha}[I_o + n_0] + \sigma} \geq \overline{\gamma}, \\ & 0 \leq d_u \leq 2L, \\ & 0 \leq d_v \leq 2L \end{aligned} \tag{44}$$

where $p_r(d_u, d_v, d_{u,v})$, I_v, I_o and σ are expressed as

$$p_r\big(d_u, d_v, d_{u,v}\big) = 1 - F_Y\left(2^{\frac{Z}{T - \sum_{i \in \mathcal{M}} \tau_i(V)}} - 1\right), \tag{45}$$

$$k_1 = \frac{P_0 d_u^{-\alpha}}{I_v + n_0},$$

$$k_2 = \frac{P_0 d_v^{-\alpha}}{I_o + n_0}$$

$$I_v = \sum_{u=1}^{2|F|} \left|H^i_{u,v}\right|^2 P_0 K d^{-\alpha}_{u,v} \tag{46}$$

$$I_o = \sum_{u=1}^{2|F|} \left|H^j_{v,u}\right|^2 P_0 K d^{-\alpha}_{v,u} \tag{47}$$

$$\sigma \triangleq \frac{(I_v + n_0)(I_o + n_0)}{P_0 K} \tag{48}$$

According to the definition of convex optimization [30], **P3** is a convex optimization problem. Since the objective function and other inequality constraints are affine functions, according to Slatter's theory [31], the Karush-Kuhn-Tucker (KKT) conditions are necessary and sufficient conditions for the optimal solution to problem (46). We can obtain the approximate optimal solution by applying the KKT optimality conditions and the Lagrange multiplication method. For this purpose, the Lagrange function is given by

$$\begin{aligned} &\mathcal{L}\big(d_u, d_v, d_{u,v}, \pi_1, \pi_2, \pi_3, \pi_4\big) \\ &= \sum_{\substack{u,v \in \mathcal{V} \\ i,j \in \mathcal{E}}} (I_v + I_o) + \pi_1\big[p_r\big(d_u, d_v, d_{u,v}\big) s_{u,v}(\boldsymbol{\Omega}) - \overline{p}\big] \end{aligned}$$

$$+\ \pi_2\left(\frac{P_0 K d_u^{-\alpha} d_v^{-\alpha}}{d_u^{-\alpha}[I_v+n_0]+d_v^{-\alpha}[I_o+n_0]+\sigma}-\overline{\gamma}\right)$$
$$+\ \pi_3(2L-d_u)+\pi_4(2L-d_v) \tag{49}$$

where π_1, π_2, π_3 and π_4 are nonnegative Lagrange multipliers. The dual approach thus results in an elegant decomposition of the original problem. We introduce a dual function as follows:

$$\begin{aligned}\max_{\pi_1,\pi_2,\pi_3,\pi_4}\ \min_{d_u,d_v,d_{u,v}}\ & \mathcal{L}\big(d_u,d_v,d_{u,v},\pi_1,\pi_2,\pi_3,\pi_4\big)\\ \text{s.t.}\ & p_r\big(d_u,d_v,d_{u,v}\big)s_{u,v}(\boldsymbol{\Omega})\geq\overline{p},\\ & \frac{P_0 K d_u^{-\alpha} d_v^{-\alpha}}{d_u^{-\alpha}[I_v+n_0]+d_v^{-\alpha}[I_o+n_0]+\sigma}\geq\overline{\gamma},\\ & 0\leq d_u\leq 2L,\\ & 0\leq d_v\leq 2L.\end{aligned} \tag{50}$$

As a result, the original optimization problem satisfies duality, which can be expressed as

$$\max_{\pi_1,\pi_2,\pi_3,\pi_4}\min_{d_u,d_v,d_{u,v}}\ \mathcal{L}=\min_{d_u,d_v,d_{u,v}}\max_{\pi_1,\pi_2,\pi_3,\pi_4}\ \mathcal{L} \tag{51}$$

Thus, the duality holds such that the globally optimal solution to (46) satisfies the KKT conditions, which are expressed as follows:

$$\begin{cases}\frac{\partial\mathcal{L}}{\partial d_{u,v}}=0\\ \frac{\partial\mathcal{L}}{\partial d_u}=0\\ \frac{\partial\mathcal{L}}{\partial d_v}=0\\ \pi_1\big[p_r\big(d_u,d_v,d_{u,v}\big)s_{u,v}(\boldsymbol{\Omega})-\overline{p}\big]=0\\ \pi_2\left(\frac{P_0 K d_u^{-\alpha} d_v^{-\alpha}}{d_u^{-\alpha}[I_v+n_0]+d_v^{-\alpha}[I_o+n_0]+\sigma}-\overline{\gamma}\right)=0\\ \pi_3(2L-d_u)\geq 0\\ \pi_4(2L-d_v)\geq 0\end{cases} \tag{52}$$

The optimal distance between nodes in $\boldsymbol{G}_{LIDG}=(\mathcal{V},\mathcal{E})$ is given by (53) as shown at the bottom of the page, where ℓ is the iteration index. Similarly, the optimal distance between nodes in $\boldsymbol{G}_{LIDG}=(\mathcal{V},\mathcal{E})$ can be expressed as

$$d_u^{\ell}=\left[\sqrt[\alpha]{\frac{\left\{d_v^{\ell-1}\right\}^{-\alpha}\left(\sqrt{KP_0\overline{p}\pi_2\pi_3\left\{d_{u,v}^{\ell-1}\right\}^{-\alpha}}-\pi_3\right)}{\overline{\gamma}\pi_3}}\right]^{+} \tag{54}$$

$$d_v^{\ell}=\left[\sqrt[\alpha]{\frac{\left\{d_u^{\ell-1}\right\}^{-\alpha}\left(\sqrt{KP_0\overline{p}\pi_2\pi_4\left\{d_{u,v}^{\ell-1}\right\}^{-\alpha}}-\pi_4\right)}{\overline{\gamma}\pi_4}}\right]^{+} \tag{55}$$

Additionally, the remaining Lagrange multipliers can be updated in accordance with the gradient descent method [32], as follows:

$$\begin{cases}\pi_1^{\ell+1}=\pi_1^{\ell}-\xi_1\big[\,p_r\big(d_u,d_v,d_{u,v}\big)s_{u,v}(\boldsymbol{\Omega})-\overline{p}\big]^{+}\\ \pi_2^{\ell+1}=\pi_2^{\ell}-\xi_2\left[\frac{P_0 K d_u^{-\alpha} d_v^{-\alpha}}{d_u^{-\alpha}[I_v+n_0]+d_v^{-\alpha}[I_o+n_0]+\sigma}-\overline{\gamma}\right]^{+}\\ \pi_3^{\ell+1}=\pi_3^{\ell}-\xi_3[2L-d_u]^{+}\\ \pi_4^{\ell+1}=\pi_4^{\ell}-\xi_4[2L-d_v]^{+}\end{cases} \tag{56}$$

where ξ_1, ξ_2, ξ_3 and ξ_4 are positive step lengths. The iterative process is guaranteed to converge to yield an approximately optimal solution when these step sizes are sufficiently small.

Since the approximately optimal solution must be obtained via an iterative approach, we design an iterative algorithm, named the iteration algorithm for multiuser cooperative mobility, to represent the execution process of the equations and the implemented entities, which is elaborated in **Algorithm 1**.

In the first stage of Algorithm 1 (lines 1-4), $\boldsymbol{G}_{LIDG}=(\mathcal{V},\mathcal{E})$ as defined in Definition 1 is derived from the input data (the communication graph and the CSI), and then, the parameters and control thresholds of the iterative process are initialized. In the second stage (lines 6-19), the objective parameters ($d_{u,v}^{\ell}$, d_u^{ℓ} and d_v^{ℓ}) and Lagrange multipliers are iteratively updated until $\ell>\ell_{\max}$. During the iterative process, a judgment condition aims to ensure that the difference between the objective parameters and the optimal solution is sufficiently small to approximate the optimal solution. Finally, the algorithm outputs the final optimal distances $d_{u,v}^{*}$, d_u^{*} and d_v^{*} in the LIDG, from which the optimal position coordinates of the RUDs in the communication graph can be determined.

Lines 5-21 will be executed $\lceil\ell_{\max}\rceil$ times. Additionally, lines 16-20 will be executed $\lceil\max\{\log_2\frac{d_{u,v}^{\ell}}{\vartheta_{u,v}},\log_2\frac{d_u^{\ell}}{\vartheta_u},\log_2\frac{d_v^{\ell}}{\vartheta_v}\}\rceil$ times, where $\vartheta_{u,v}$, ϑ_u and ϑ_v denote control thresholds. Note that the distances between nodes are less than $2L$ in each iteration, i.e.,

$$d_{u,v}^{\ell}=\left[\sqrt[\alpha]{\frac{e^{\frac{-0.5\lambda Z}{T-\sum_{i\in\mathcal{M}}\tau_i(V)}}\left(\Psi_1\left(1-\frac{Z}{T-\sum_{i\in\mathcal{M}}\tau_i(V)}\right)-\sqrt{\Psi_2\left(\left\{d_u^{\ell-1}\right\}^{-\alpha}+\left\{d_v^{\ell-1}\right\}^{-\alpha}\right)}\right)}{\left(2^{\frac{Z}{T-\sum_{i\in\mathcal{M}}\tau_i(V)}}-1\right)\eta\left(2d_u^{\ell-1}+2d_v^{\ell-1}+KP_0\pi_2 d_u^{\ell-1}d_v^{\ell-1}\right)-\overline{\gamma}}}\right]^{+}$$
$$\Psi_1\triangleq 2P_0\overline{p}\eta\left(d_u^{\ell-1}+d_v^{\ell-1}\right)$$
$$\Psi_2\triangleq P_0\pi_1\eta s_{u,v}(\boldsymbol{\Omega}) \tag{53}$$

Algorithm 1: Iteration Algorithm for Multiuser Cooperative Mobility

Input: Communication graph $\boldsymbol{G}_p = (\mathcal{H}, E)$ and channel state information (CSI).

1 Convert $\boldsymbol{G}_p = (\mathcal{H}, E)$ into $\boldsymbol{G}_{LIDG} = (\mathcal{V}, \mathcal{E})$ in accordance with **Definition 1** and then obtain $d_{u,v}^{(0)}$, $d_u^{(0)}$ and $d_v^{(0)}$ in $\boldsymbol{G}_{LIDG} = (\mathcal{V}, \mathcal{E})$;
2 Initialize $\ell = 0$ and the Lagrange multipliers π_1^0, π_2^0, π_3^0 and π_4^0;
3 Initialize the maximum number of iterations $\ell_{\max}$ [33] and the control thresholds $\vartheta_{u,v}$, ϑ_u and ϑ_v;
4 Let $d_{u,v}^* = d_{u,v}^{(0)}$, $d_{u,v}^* = d_{u,v}^{(0)}$ and $d_{u,v}^* = d_{u,v}^{(0)}$;
5 **while** $\ell \leqslant \ell_{\max}$ **do**
6 **if** $\ell + 1 > \ell_{\max}$ **then**
7 $d_{u,v}^* = d_{u,v}^{\ell}$;
8 $d_u^* = d_u^{\ell}$;
9 $d_v^* = d_v^{\ell}$;
10 **else**
11 Update $d_{u,v}^{\ell}$ using (53);
12 Update d_u^{ℓ} using (54);
13 Update d_v^{ℓ} using (55);
14 Update the Lagrange multipliers π_1^{ℓ}, π_2^{ℓ}, π_3^{ℓ} and π_4^{ℓ} using (56);
15 **end**
16 **if** $\{d_{u,v}^{\ell} - d_{u,v}^{\ell-1} < \vartheta_{u,v}\}\&\&\{d_u^{\ell} - d_u^{\ell-1} < \vartheta_u\}\&\&\{d_v^{\ell} - d_v^{\ell-1} < \vartheta_v\}$ **then**
17 $d_{u,v}^* = d_{u,v}^{\ell}$;
18 $d_u^* = d_u^{\ell}$;
19 $d_v^* = d_v^{\ell}$;
20 **end**
21 **end**

Output: $d_{u,v}^*$, d_u^* and d_v^*.

$\max\{d_u^{\ell}, d_v^{\ell}\} \leq 2L$. This implies that lines 16-20 should be executed $\lceil \max\{\log_2 \frac{d_{u,v}^{\ell}}{\vartheta_{u,v}}, \log_2 \frac{2L}{\vartheta_u}, \log_2 \frac{2L}{\vartheta_v}\} \rceil$ times. However, due to lines 7-11, the worst-case complexity of this algorithm is $\lceil \ell_{\max} \rceil$ executions. Thus, the complexity of **Algorithm 1** is $\mathcal{O}(\ell_{\max})$. If $\ell_{\max}$ is too large, the complexity of the algorithm is too high; if it is too small, then the accuracy of the solution will not be sufficient to approximate the optimal solution. Therefore, to achieve a desirable tradeoff, we set $\ell_{\max}$ in the range of $[10^5, 10^6]$ in the following simulation study [33].

Although Algorithm 1 describes the method of calculating the optimal locations of the relay nodes in detail, the multiuser cooperative mobility process for the RUDs has not been elaborated. To facilitate its description, we present a vivid example for illustration in Fig. 6. Initially, three RUDs, A, B and C, are randomly distributed in a limited circular active area divided into four blocks. Thus, we can roughly record the RUDs' position coordinates in accordance with the distribution of the blocks. As shown in Fig. 6(1), A, B, and C are located in three different blocks, denoted by

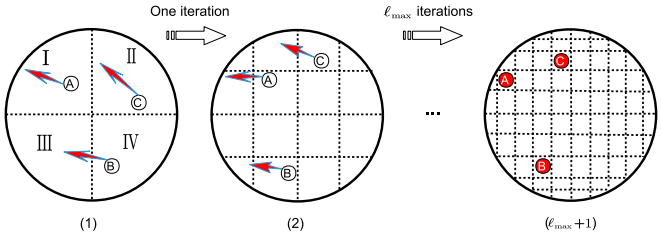

FIGURE 6. Iteration of the multiuser cooperative mobility process involved three RUDs (A, B, C).

$\boldsymbol{U}_A = \{\text{I}\}$, $\boldsymbol{U}_B = \{\text{IV}\}$ and $\boldsymbol{U}_C = \{\text{III}\}$. Fig. 6(2) depicts that in the next iteration, the number of blocks increases exponentially, with an exponent of 2, to sixteen, and the positions of the RUDs are also updated based on the algorithm. By the $\ell_{\max}^{th}$ iteration, the number of blocks is $2^{2\ell_{\max}}$, and these nodes have moved to their optimal positions, at which point the positions of the small blocks are the final coordinate representations of each node.

C. OVERALL ALGORITHM

In this section, the overall RS-LIDG algorithm is proposed, which combines the relay selection scheme and the user cooperative mobility strategy as follows.

As described in **Algorithm 2**, the selection variables and parameters are first initialized, and potential RUDs are then selected from among the feasible MUDs whose social intimacy values are larger than a predefined threshold (lines 1-2). Lines 3-19 describe the iterative process of selecting $|\widehat{R}|$ relays. For the selection of each relay, the instantaneous reward is compared against the expected threshold. If the instantaneous reward is larger than the threshold, this potential node is selected as a new relay; otherwise, the process of detecting potential nodes continues until the last one is detected. During this process, if no node satisfying the abovementioned constraints is selected, then the last detected node is selected as a new relay, i.e., $k^* = |M|$. Finally, as shown in lines 20-24, the best relay selection scheme $\boldsymbol{\Omega}^*$ is obtained, and the optimal MUD position coordinates $\boldsymbol{U}^*$ are determined based on **Algorithm 1**.

Now, we present a simple analysis of the complexity of our proposed RS-LIDG algorithm. The original optimization problem (27) is decomposed into two subproblems, **P1** and **P2**. The first corresponds to the relay selection scheme and is solved by identifying the optimal stopping phase; hence, the complexity is $\mathcal{O}(k^*|\widehat{R}|)$. Furthermore, the index k^* is less than or equal to the number of MUDs $|M|$, meaning that the complexity is $\mathcal{O}(|M||\widehat{R}|)$ in the worst case. As a result, the computational complexity of the proposed algorithm is $\mathcal{O}(\max\{\ell_{\max}, |M||\widehat{R}|\})$.

VI. SIMULATION AND PERFORMANCE ANALYSIS

In this section, the proposed algorithm is evaluated and compared with five conventional algorithms in terms of throughput performance and complexity.

Algorithm 2: RS-LIDG Algorithm

Input: Communication graph $\boldsymbol{G}_p = (\mathcal{H}, E)$, social intimacy graph $\boldsymbol{G}_s = \{\mathcal{H}, \mathcal{S}\}$, channel gain information (CSI known).

Select feasible MUDs with social intimacy greater than the predefined threshold $\bar{s}$ as potential relays in $\boldsymbol{G}_s = \{\mathcal{H}, \mathcal{S}\}$;
Initialize the number of selected RUDs $j = 0$, the set of selected RUDs $\Re = \{\oslash\}$, and the stopping phase index $k = 0$;
while $j = |F|$ **do**
  Calculate the thresholds Ξ_k^* using (34);
  Calculate the instantaneous reward $\Phi_{eff}^k\big(T, \tau_{m(k)}\boldsymbol{\Omega}\big(m_{(k)}\big)\big)$ using (31);
  if $\Phi_{eff}^k\big(T, \tau_{m(k)}\boldsymbol{\Omega}\big(m_{(k)}\big)\big) < \Xi_k^*$ **then**
    Go back to step (5);
    if $|k| < |M|$ **then**
      $k = k + 1$;
    else
      Select the RUD with index $|M|$ as a new relay;
      Go to step (16);
    end
  else
    Select the RUD with index k^* as a new relay;
    $\Re = \Re \cup \{k^*\}$;
  end
  $j = j + 1$;
end
Map to the indicator function $\boldsymbol{\Omega}^*$ based on the index of set $\Re$, where $\exists m_i = \mathbf{1}$, $i = k^* \in \Re$;
Obtain the indicator function $\boldsymbol{\Omega}^*$ using (37);
Obtain $d_{u,v}^*$, d_u^* and d_v^* using Algorithm 1;
Obtain the optimal MUD position coordinates $\boldsymbol{U}^*$ based on $d_{u,v}^*$, d_u^* and d_v^*;
Calculate the optimal throughput Th_{sys}^* using (19);

Output: $\boldsymbol{\Omega}^*$, $\boldsymbol{U}^*$, and Th_{sys}^*.

- *Intuitive Method (IM) [9]:* A mobile relay with sufficient social intimacy moves along a link to the midpoint location between the transmitter and receiver.
- *Direct Transmission (DT):* As the name implies, direct D2D communication does not require any relay; instead, communication is sent directly from the AP to the receiver. However, considering the channel fading and distance factors, this method's performance is relatively low and can serve as a benchmark reference.
- *Social-Trust-Based Selection and Random Mobility (STS-RM) [6]:* Relays are selected on the basis of the inherent social intimacy between users, regardless of the physical-layer characteristics. The selected RUDs move randomly within the limited circular mobility space.

TABLE 3. Parameter values for simulation.

Parameter	Value
Communication standard	IEEE 802.11g [34]
Number of FUDs ($\|F\|$)	10
Transport protocol	UDP
Path-loss exponent (α)	4.00
Path-loss constant (K)	1.00
Maximum D2D transmission power	10 dBm
White Gaussian Noise (N_0)	-90 dBm
D2D decoding threshold ($\overline{\gamma}$)	20 dB
Initial social intimacy threshold ($\overline{s}$)	0.4
Initial link reliability threshold ($\overline{p}$)	0.5
Wave frequency	2.4 GHz
System bandwidth ($\mathscr{B}$)	10 MHz
Rayleigh fading standard deviation (Ω)	8 dB

- *Physical-Based Selection and Random Mobility (PHS-RM) [7]:* Relays are selected on the basis of the interference and SINR between users, regardless of the social-layer characteristics. Subsequently, the selected RUDs also move randomly.
- *Random Selection and Random Mobility (RS-RM):* The controller randomly selects a relay without detection or valid algorithm checks. The cooperative mobility of the RUDs is also haphazard, without any explicit strategy.

A. NETWORK PARAMETER SETTINGS

In this ad hoc network, the activity scope of the RUDs is a circular area with radius L. The FUDs and AP are located on either side of this circular area, and the devices' initial coordinates follow a random distribution. Considering the actual mobility distance and relay requirements, we set L to range from 100 m to 200 m. Since the randomness of the initial locations may affect the results, we conducted more than 1,000 experiments and summarized the resulting statistics. Additionally, since social relationships vary with social domains and inherent trust, we set the link reliability threshold $\overline{p}$ to range from 0 to 1. We defined the mobility velocity for each RUD to be 1.5 m/s, which is the average speed of a pedestrian. Recall that our goal is to find the best selected relays and the optimal positions for cooperative mobility; hence, the mobility velocity will not affect the final throughput result. The variance of the exponential distribution in Rayleigh fading channels was considered to be 8 dB or 10 dB, so $\lambda = 0.4$ and $\eta = 0.9$, and we set $\frac{Z}{T_{eff}}$ to 7.5 [35]. We set the random variable of contact durations T to follow the gamma distribution $G_T \sim Gamma(4.43, \frac{1}{1088})$ [36]. The detailed configuration of the simulation parameters is shown in Table 3.

B. THROUGHPUT PERFORMANCE ANALYSIS

First, we evaluate our proposed RS-LIDG algorithm's throughput performance by comparing it with the above five conventional methods. Fig. 7 shows the system throughput

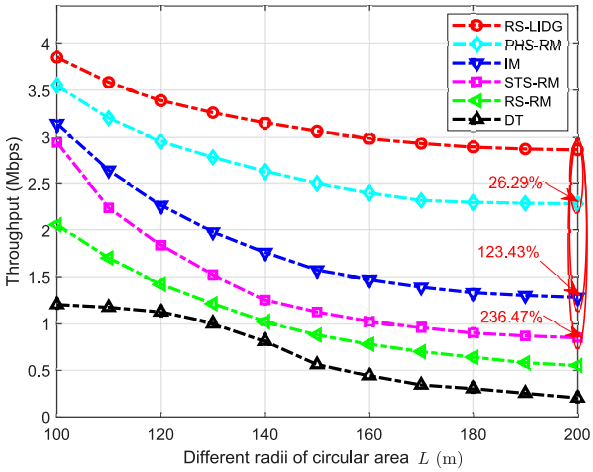

FIGURE 7. System throughput comparison under the different radius of the mobile circular area *L*.

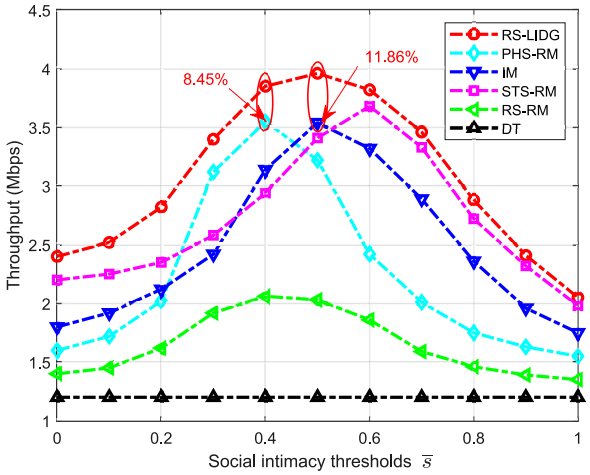

FIGURE 8. System throughput comparison under different social intimacy thresholds $\bar{s}$.

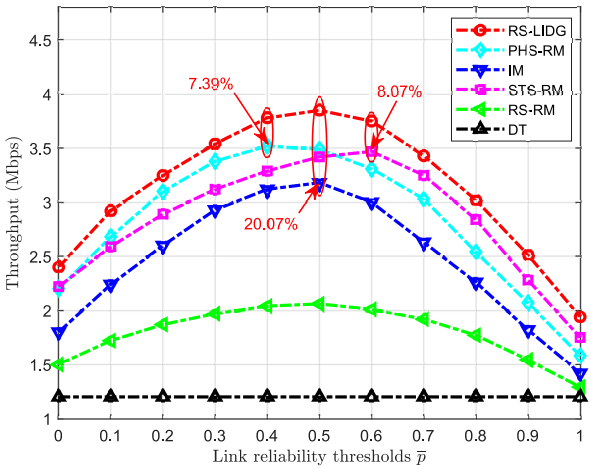

FIGURE 9. System throughput comparison under different link reliability thresholds $\bar{p}$.

obtained as the harmonic mean of all users' effective transmission rates, where $|M| = 20$, $\bar{s} = 0.4$ and $\bar{p} = 0.5$. From these results, one can observe that the throughput decreases as the mobility area's radius L increases for all six algorithms. For the DT method, the curve drops rapidly from 100 m to 140 m and then tends to stabilize up to 200 m. This is because a larger L leads to stronger channel fading and lower received power for direct transmission. In contrast to that for DT, the curves for the other algorithms decline more smoothly, and our proposed algorithm shows the least degradation in throughput performance. The reason is that the number of available trunks per unit area is reduced; meanwhile, both the SINR and transmission rate are increased due to the relay selection scheme and user mobility, leading to positive feedback. Compared with PHS-RM, IM, and STS-RM, the proposed RS-LIDG algorithm achieves maximum throughput improvements of 26.29%, 123.43%, and 236.47%, respectively.

Fig. 8 and Fig. 9 evaluate the impact of different social intimacy thresholds $\bar{s}$ and link reliability thresholds $\bar{p}$ on the system throughput, both of which are concave functions for all algorithms. As illustrated Fig. 8, the proposed RS-LIDG algorithm improves the throughput by 11.86% and 8.45% compared to IM and PHS-RM, respectively, where $L = 100$ m, $|M| = 20$ and $\bar{p} = 0.5$. For RS-LIDG and IM, the throughput reaches a maximum of $\bar{s} = 0.4$. For PHS-RM and STS-RM, the maximum points lie at $\bar{s} = 0.4$ and $\bar{s} = 0.6$. As illustrated in Fig. 9, the proposed RS-LIDG algorithm improves the throughput by 20.07%, 8.07% and 7.39% at the maximum points compared to IM, STS-RM and PHS-RM, respectively, where $L = 100$ m, $|M| = 20$ and $\bar{s} = 0.4$.

This is because RUDs with low intimacy and low transmission success rates are eliminated while also ensuring the link reliability, resulting in an increase in the effective transmission time and SINR of each relay. After the peak point, the number of available MUDs is reduced such that a longer time is needed to select favorable relays while also incurring a reduction in link reliability. For RS-RM and DT, it can be seen that both $\bar{s}$ and $\bar{p}$ have little or no effect on the throughput. The reason is that due to the absence of relays or the random nature of the relay selection process, social attributes have almost no impact on throughput in either scenario.

Fig. 10 depicts the impact of different numbers of MUDs $|M|$ on the throughput, where $L = 100$ m and $\bar{s} = 0.4$. It can be observed that the throughput curves are increasing functions of $|M|$. We also observe that our proposed RS-LIDG algorithm achieves higher throughput than the other methods. The reasons are as follows. As the number of MUDs that can be selected grows, the probability of selecting an effective relay increases, allowing the transmission links selected for relaying to be stable, which effectively improves the transmission time and throughput. On the other hand, since the proposed method considers both physical and social constraints, the cooperative multiuser mobile strategy can effectively reduce user interference and improve the

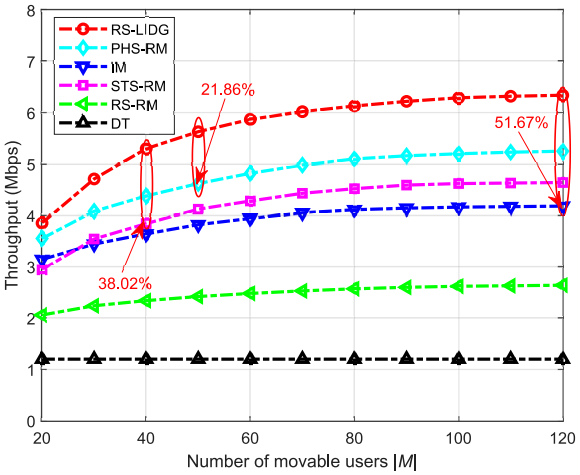

FIGURE 10. System throughput comparison under different numbers of MUDs $|M|$.

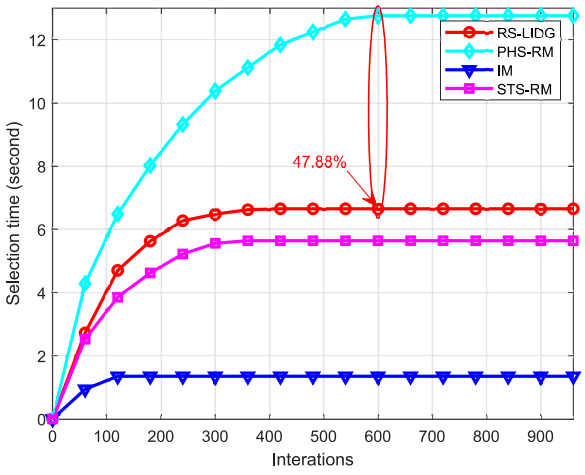

FIGURE 11. Comparison of system throughput during iterations.

SINR. Finally, compared with PHS-RM, STS-RM, and IM, the throughput of RS-LIDG is increased by 21.86%, 38.02%, and 51.67%, respectively.

C. RELAY SELECTION COST AND ALGORITHM COMPLEXITY ANALYSIS

In addition to evaluating the throughput performance, we also need to consider the relay selection cost and algorithm complexity. Fig. 11 shows a comparison of the system throughput throughout the iterative process. Note that the CPU of the computer used for simulation was an Intel Core i7-8700 3.20 GHz. It can be seen from Fig. 10 that RS-LIDG reduces the relay selection time by 47.88% compared to PHS-RM. From the column chart in Figure 12, we can see that the RS-LIDG algorithm is faster than PHS-RM and close to STS-RM in terms of relay selection time.

This, in essence, can be attributed to the proposed relay selection scheme, particularly the calculation of the optimal stopping phase based on an instantaneous payoff greater than a preset threshold, while the process of preselecting potential RUDs guarantees that the social intimacy constraints are met. On the other hand, as expected, the complexity of the proposed multiuser cooperative mobility strategy, i.e., Algorithm 1, is relatively low, validating our algorithm complexity analyses above ($\mathcal{O}(\max\{\ell_{\max}, |M||\widehat{R}|\})$).

D. COMMUNICATION OVERHEAD ANALYSIS

In a real network, the communication overhead of algorithm execution has a significant impact on the actual amount of data transferred. Here, the percentage of redundant data in the total is set as an evaluation indicator of the communication overhead, which consists of control information, user's location information, and valid policy information. The comparison of communication overhead among STS-RM, PHS-RM, and RS-LIDG is depicted in Fig. 13, where X-axis represents the computational time cost and Y-axis denotes the percentage of redundant data in total transferred. Therefore, the communication overhead is the area enclosed

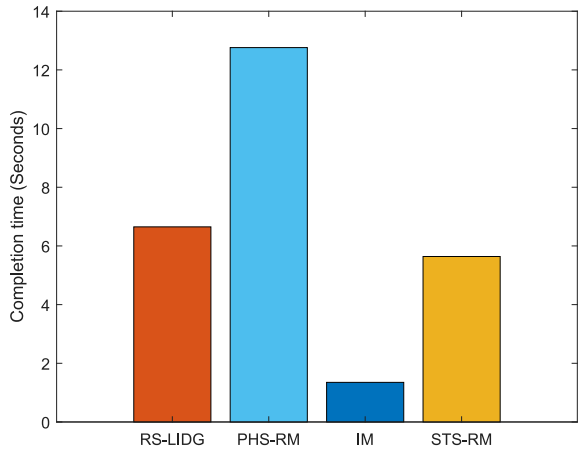

FIGURE 12. Comparison histogram of system throughput for four algorithms: RS-LIDG, PHS-RM, IM, and STS-RM.

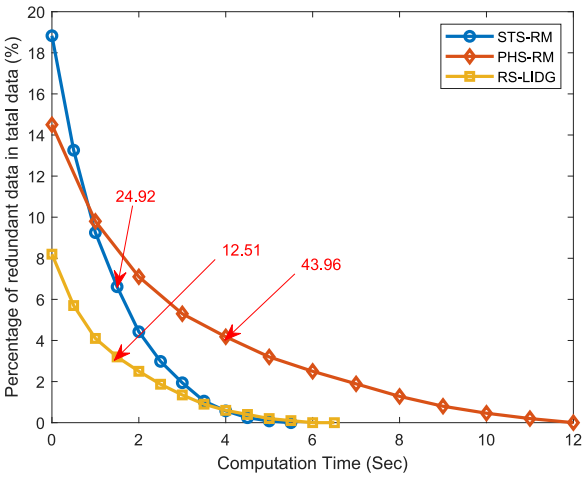

FIGURE 13. Comparison histogram of system throughput for four algorithms: RS-LIDG, PHS-RM, IM, and STS-RM.

by the curve and the X-axis, whose value is equal to the definite integral in a finite computation time.

We observe that the curve gradually decreases and finally converges to zero at the maximum computation time. The

reason is that the control strategies and location information required by these algorithms are degressive until the relay selection is finally confirmed. It is noted that the communication overhead of STS-RM, PHS-RM, and RS-LIDG is 24.92, 43.96, and 12.51, respectively. The results show that our proposed RS-LIDG reduces the communication overhead by 49.80% and 71.54% compared to STS-RM and PHS-RM. The main reasons are as follows: i) in the relay selection scheme, RS-LIDG only requires to select the optimal stopping phase according to the known control information, instead of traversing all phases for the traditional algorithms; ii) RS-LIDG can iteratively partition the mobility region to obtain the optimum in the multiuser cooperative mobility strategy, while the traditional algorithm must exhaustive all locations cases. Thus, STS-RM and PHS-RM require more redundant data than RS-LIDG.

VII. CONCLUSION AND FUTURE WORK

In this paper, we formulate a social-physical ad hoc network model based on multiuser cooperative mobility. The impacts of social intimacy and the probability of physical-layer data transmission success on link reliability are illustrated in this model. Accordingly, the system throughput maximization problem is constructed to optimize the selection of potential mobile relays and their geographic locations through a relay selection scheme and a cooperative mobility strategy. Moreover, we propose the Relay Selection and Link Interference Degree Graph (RS-LIDG) algorithm to address this NP-hard problem. It is proven that the proposed relay selection scheme can minimize the relay selection time while maintaining a high throughput gain. Furthermore, we define a graph representing the degrees of interference between links and verify that optimizing the mobile relays' locations with the proposed mobility strategy results in the maximization of the throughput performance. Numerical results show that our proposed RS-LIDG algorithm can increase the throughput gain by 26.29%, 123.43%, and 236.47% compared to IM, STS-RM, and PHS-RM, respectively.

Since this paper primarily focuses on the theoretically achievable throughput performance, we have adopted several useful assumptions based on system modeling and ad hoc network modeling considerations. Specifically, the current study has two limitations that can be targeted for improvement in future work.

First, we have not analyzed the data transmission loss of the relays during the mobility process of the developed model. Although the mobility time is short for existing communication systems, it does consume specific transmission slots for the relays, from disconnection to final access for the fixed users. Therefore, we need to consider this contribution to the data throughput loss.

Second, the complexity of our proposed RS-LIDG algorithm is still high, making it difficult to meet the requirements of real-time systems with high accuracy. Compared with IM, our proposed cooperative mobility strategy has much space for improvement in terms of complexity. In the future, we will address these two issues by considering the data loss during relay mobility and reducing the degree of complexity. We hope to analyze the cases in which good throughput performance can be achieved without relay movement. Thus, the critical threshold conditions for the mobility and nonmobility of the relays can be derived.

APPENDIX
PROOF OF THEOREM 2

As mentioned above, $\Xi^*_{|M|} = -\infty$ means that it is always optimal for the controller to stop detecting in the $|M|^{th}$ phase. According to (32), for the $|M-1|^{th}$ phase, we can derive $\Xi^*_{|M|-1}$ as follows:

$$\begin{aligned}\Xi^*_{|M|-1} &= \mathbb{E}\left[\Phi^{|M|}_{eff}\left(T, \tau_{m_{(|M|)}}\boldsymbol{\Omega}\left(m_{(|M|)}\right)\right)\right] \\ &= \int_{\tau}\int_{T}\Phi^{|M|}_{eff} f_{\tau T}(\tau, t)d\tau dt \\ &= (\tau_{\max}-\tau_{\min})\int_{T_{\min}}^{T_{\max}}\frac{t^{(\mu-1)}\exp^{\left(-\frac{t}{\rho}\right)}}{\Gamma(\mu)\rho^{\mu}}dt \\ &\quad - \sum|M|\int_{T_{\min}}^{T_{\max}}\int_{\tau_{\min}}^{\tau_{\max}}\tau\frac{t^{(\mu-1)}\exp^{\left(-\frac{t}{\rho}\right)}}{\Gamma(\mu)\rho^{\mu}}d\tau dt\end{aligned} \tag{57}$$

where $f_{\tau T}(\tau, t)$ is the joint PDF of $f_T(x)(\cdot)$ and $f_{\tau_{m_k}}(x)(\cdot)$. In particular, $\tau_{\max}$, $\tau_{\min}$, $T_{\max}$ and $T_{\min}$ denote the maximum and minimum values of the relay selection time and the contact durations between the AP and FUDs, respectively. Likewise, we can obtain Ξ^*_k as

$$\begin{aligned}\Xi^*_k &= \mathbb{E}\left\{\max\left[\Phi^{k+1}_{eff}\left(T, \tau_{m_{(k+1)}}\boldsymbol{\Omega}\left(m_{(k+1)}\right)\right), \Xi^*_{k+1}\right]\right\} \\ &= \mathbb{E}\left\{\Phi^{k+1}_{eff}\left(T, \tau_{m_{(k+1)}}\boldsymbol{\Omega}\left(m_{(k+1)}\right)\right)\right\}|\Delta_1 + \mathbb{E}\left\{\Xi^*_{k+1}\right\}|\Delta_2 \\ &= \iint_{\Delta_1}\Phi^{k+1}_{eff} f_{\tau T}(\tau, t)d\tau dt + \Xi^*_{k+1}\iint_{\Delta_2} f_{\tau T}(\tau, t)d\tau dt \\ &= \int_{T_{\min}}^{T_{\max}}\int_{\Xi_k}^{\tau_{\max}}\left(t - \sum|k+1|\right)\frac{1}{t}\frac{t^{(\mu-1)}e^{\left(-\frac{t}{\rho}\right)}}{\Gamma(\mu)\rho^{\mu}}d\tau dt \\ &\quad + \Xi^*_{k+1}\int_{T_{\min}}^{T_{\max}}\int_{\tau_{\min}}^{\Xi_k}\frac{1}{t}\frac{t^{(\mu-1)}e^{\left(-\frac{t}{\rho}\right)}}{\Gamma(\mu)\rho^{\mu}}d\tau dt \\ &= \left[\tau_{\max} + \left(\Xi^*_{k+1}-1\right)\Xi_k - \Xi^*_{k+1}\tau_{\min}\right] \\ &\quad \times \int_{T_{\min}}^{T_{\max}}\frac{t^{(\mu-2)}e^{\left(-\frac{t}{\rho}\right)}}{\Gamma(\mu)\rho^{\mu}}dt \\ &\quad - \sum|k+1|\int_{T_{\min}}^{T_{\max}}\int_{\Xi_k}^{\tau_{\max}}\frac{t^{(\mu-2)}e^{\left(-\frac{t}{\rho}\right)}}{\Gamma(\mu)\rho^{\mu}}d\tau dt\end{aligned} \tag{58}$$

where Δ_1 and Δ_2 denote the integral intervals under the conditions of $\Phi^{k+1}_{eff} \geq \Xi^*_{k+1}$ and $\Phi^{k+1}_{eff} < \Xi^*_{k+1}$, respectively.

REFERENCES

[1] P. Schulz *et al.*, "Latency critical IoT applications in 5G: Perspective on the design of radio interface and network architecture," *IEEE Commun. Mag.*, vol. 55, no. 2, pp. 70–78, Feb. 2017.

[2] H. Luo, R. Ramjee, P. Sinha, L. Li, and S. Lu, "UCAN: A unified cellular and ad-hoc network architecture," in *Proc. 9th Annu. Int. Conf. Mobile Comput. Netw.*, 2003, pp. 353–367.
[3] G. J. Sutton *et al.*, "Enabling technologies for ultra-reliable and low latency communications: From PHY and MAC layer perspectives," *IEEE Commun. Surveys Tuts.*, vol. 21, no. 3, pp. 2488–2524, 3rd Quart., 2019.
[4] T. Igarashi, J. Takai, and T. Yoshida, "Gender differences in social network development via mobile phone text messages: A longitudinal study," *J. Social Pers. Relationships*, vol. 22, no. 5, pp. 691–713, 2005.
[5] R. Jurdak, C. V. Lopes, and P. Baldi, "A survey, classification and comparative analysis of medium access control protocols for ad hoc networks," *IEEE Commun. Surveys Tuts.*, vol. 6, no. 1, pp. 2–16, 1st Quart., 2004.
[6] M. Zhang, X. Chen, and J. Zhang, "Social-aware relay selection for cooperative networking: An optimal stopping approach," in *Proc. IEEE Int. Conf. Commun.*, 2014, pp. 2257–2262.
[7] X. Pan and H. Wang, "On the performance analysis and relay algorithm design in social-aware D2D cooperated communications," in *Proc. IEEE Veh. Technol. Conf.*, Jul. 2016, pp. 1–5.
[8] Z. Fang and X. Li, "A novel relay selection algorithm based on mobile social networks for device-to-device cooperative communications," in *Proc. 13th Int. Conf. Nat. Comput. Fuzzy Syst. Knowl. Disc. (ICNC-FSKD)*, 2018, pp. 2755–2761.
[9] U. S. Khwakhali, S. Gordon, and P. Suksompong, "Social-Aware relay selection for device to device communications in cooperative cellular networks," in *Proc. Int. Electr. Eng. Congr. (iEECON)*, 2017, pp. 9–12.
[10] H. Mao, W. Feng, and N. Ge, "Performance of social-position relationships based cooperation among mobile terminals," *IEEE Trans. Veh. Technol.*, vol. 65, no. 5, pp. 3128–3138, May 2016.
[11] H. Zhang, Q. Du, P. Ren, and Z. Wang, "Social stability enhanced mobile D2D relay networks: An optimal stopping approach," in *Proc. IEEE Int. Conf. Commun.*, 2017, pp. 1–6.
[12] J. Xie and T. Murase, "Multiple user cooperative mobility in mobile ad hoc networks: An interaction position game.," *IEEE Access*, vol. 8, pp. 126297–126314, 2020.
[13] J. Xie and T. Murase, "An optimal location allocation by multiuser cooperative mobility for maximizing throughput in MANETs.," *IEEE Access*, vol. 8, pp. 226089–226107, 2020.
[14] M. Grossglauser and D. N. C. Tse, "Mobility increases the capacity of ad hoc wireless networks," *IEEE/ACM Trans. Netw.*, vol. 10, no. 4, pp. 477–486, Aug. 2002.
[15] B. Baron, P. Spathis, M. D. de Amorim, Y. Viniotis, and M. H. Ammar, "Mobility as an alternative communication channel: A survey," *IEEE Commun. Surveys Tuts.*, vol. 21, no. 1, pp. 289–314, 1st Quart., 2019.
[16] T. Murase, "User cooperative mobility for better multimedia communication quality," in *Proc. ACM SIGCOMM Workshop Future Human-Centric Multimedia Netw.*, 2013, pp. 39–40.
[17] A. Chaintreau, P. Hui, J. Crowcroft, C. Diot, R. Gass, and J. Scott, "Impact of human mobility on opportunistic forwarding algorithms," *IEEE Trans. Mobile Comput.*, vol. 6, no. 6, pp. 606–620, Jun. 2007.
[18] S. Miyata, T. Murase, and K. Yamaoka, "Novel access-point selection for user QoS and system optimization based on user cooperative moving," *IEICE Trans. Commun.*, vol. E95-B, no. 6, pp. 1953–1964, 2012.
[19] T. Luo and T. Murase, "User cooperative mobility for QoS improvement in ad-hoc networks," in *Proc. 14th IEEE Annu. Consum. Commun. Netw. Conf. (CCNC)*, 2017, pp. 276–279.
[20] K. Okumura and T. Murase, "User cooperative mobility with optimal node selection for high throughput in multiple ad-hoc networks," in *Proc. 14th Int. Conf. Ubiquitous Inf. Manag. Commun. (IMCOM)*, 2020, pp. 1–7.
[21] M. Heusse, F. Rousseau, G. Berger-Sabbatel, and A. Duda, "Performance anomaly of 802.11b," in *Proc. IEEE INFOCOM*, Mar. 2003, pp. 836–843.
[22] A. Fathi, Q. Shafiee, and H. Bevrani, "Robust frequency control of microgrids using an extended virtual synchronous generator," *IEEE Trans. Power Syst.*, vol. 33, no. 6, pp. 6289–6297, Nov. 2018.
[23] Y. Li, S. Qiang, X. Zhuang, and O. Kaynak, "Robust and adaptive backstepping control for nonlinear systems using RBF neural networks," *IEEE Trans. Neural Netw.*, vol. 15, no. 3, pp. 693–701, May 2004.
[24] A. P. Aguiar and J. P. Hespanha, "Trajectory-tracking and path-following of underactuated autonomous vehicles with parametric modeling uncertainty," *IEEE Trans. Autom. Control*, vol. 52, no. 8, pp. 1362–1379, Aug. 2007.
[25] S. P. Weber, J. G. Andrews, X. Yang, and G. De Veciana, "Transmission capacity of wireless ad hoc networks with successive interference cancellation," *IEEE Trans. Inf. Theory*, vol. 53, no. 8, pp. 2799–2814, Aug. 2007.
[26] Y. Ma, G. Zhou, and S. Wang, "WiFi sensing with channel state information: A survey," *ACM Comput. Surveys*, vol. 52, no. 3, pp. 1–36, 2019.
[27] S. Berger, M. Kuhn, A. Wittneben, T. Unger, and A. Klein, "Recent advances in amplify-and-forward two-hop relaying," *IEEE Commun. Mag.*, vol. 47, no. 7, pp. 50–56, Jul. 2009.
[28] Z. Zhang, P. Zhang, D. Liu, and S. Sun, "SRSM-based adaptive relay selection for D2D communications," *IEEE Internet Things J.*, vol. 5, no. 4, pp. 2323–2332, Aug. 2018.
[29] S. Nam, M. Vu, and V. Tarokh, "Relay selection methods for wireless cooperative communications," in *Proc. 42nd Annu. Conf. Inf. Sci. Syst.*, 2008, pp. 859–864.
[30] S. Boyd and L. Vandenberghe, *Convex Optimization*. Cambridge, U.K.: Cambridge Univ. Press, 2004.
[31] S. Dempe, "Directional differentiability of optimal solutions under Slater's condition," *Math. Program.*, vol. 59, no. 1, pp. 49–69, 1993.
[32] S. Ruder, "An overview of gradient descent optimization algorithms," 2016. [Online]. Available: arXiv1609.04747.
[33] Q. Wei, D. Liu, and H. Lin, "Value iteration adaptive dynamic programming for optimal control of discrete-time nonlinear systems," *IEEE Trans. Cybern.*, vol. 46, no. 3, pp. 840–853, Mar. 2016.
[34] *Wireless LAN Medium Access Control (MAC) and Physical Layer (PHY) Specifications*, IEEE Standard 802.11g-2003, 2003.
[35] L. Wang, H. Tang, and M. Čierny, "Device-to-device link admission policy based on social interaction information," *IEEE Trans. Veh. Technol.*, vol. 64, no. 9, pp. 4180–4186, Sep. 2015.
[36] A. Passarella and M. Conti, "Analysis of individual pair and aggregate intercontact times in heterogeneous opportunistic networks," *IEEE Trans. Mobile Comput.*, vol. 12, no. 12, pp. 2483–2495, Dec. 2013.

JIQUAN XIE (Graduate Student Member, IEEE) received the B.S. and M.S. degrees from the University of Electronic Science and Technology of China, Chengdu, China, in 2013 and 2016, respectively. He is currently pursuing the Ph.D. degree with the Department of Information Engineering, Nagoya University, Nagoya, Japan. His research interests include the mobile ad hoc networking, mobile cloud computing, and edge computing.

TUTOMU MURASE (Member, IEEE) was born in Kyoto, Japan, in 1961. He received the M.E. degree from the Graduate School of Engineering Science, Osaka University, Japan, in 1986, and the Ph.D. degree from the Graduate School of Information Science and Technology, Osaka University in 2004.

He joined NEC Corporation, Japan, in 1986. He was a Visiting Professor with the Tokyo Institute of Technology from 2012 to 2014. He is currently a Professor with Nagoya University, Japan. He has more than 90 registered patents including several international patents. He has been engaged in research on traffic management for high-quality and high-speed Internet. His current interests include transport and session layer traffic control, wireless network resource management, and network security. He is also interested in user cooperative mobility research.

Prof. Murase received the Best Tutorial Paper Award on his invited paper about QoS control for overlay networks in the *IEICE Transactions on Communications* in 2006. He has served as a TPC for many IEEE conferences and workshops. He was a Secretary of the IEEE Communications Society Japan Chapter. He is a fellow of IEICE.